Coronin Promotes the Rapid Assembly and Cross-linking of Actin Filaments and May Link the Actin and Microtubule Cytoskeletons in Yeast

Bruce L. Goode,* Jonathan J. Wong,* Anne-Christine Butty,‡ Matthias Peter,‡ Ashley L. McCormack,§ John R. Yates,§ David G. Drubin,* and Georjana Barnes*

*Department of Molecular and Cell Biology, University of California, Berkeley, California 94720-3202; ‡Swiss Institute for Experimental Cancer Research, Lausanne, Switzerland; and §Department of Molecular Biotechnology, University of Washington, Seattle, Washington 98195

Abstract. Coronin is a highly conserved actin-associated protein that until now has had unknown biochemical activities. Using microtubule affinity chromatography, we coisolated actin and a homologue of coronin, Crn1p, from *Saccharomyces cerevisiae* cell extracts. Crn1p is an abundant component of the cortical actin cytoskeleton and binds to F-actin with high affinity (K_d 6×10^{-9} M). Crn1p promotes the rapid barbed-end assembly of actin filaments and cross-links filaments into bundles and more complex networks, but does not stabilize them. Genetic analyses with a *crn1Δ* deletion mutation also are consistent with Crn1p regulating filament assembly rather than stability. Filament cross-linking depends on the coiled coil domain of Crn1p, suggesting a requirement for Crn1p dimerization. As-

sembly-promoting activity is independent of cross-linking and could be due to nucleation and/or accelerated polymerization. Crn1p also binds to microtubules in vitro, and microtubule binding is enhanced by the presence of actin filaments. Microtubule binding is mediated by a region of Crn1p that contains sequences (not found in other coronins) homologous to the microtubule binding region of MAP1B. These activities, considered with microtubule defects observed in *crn1Δ* cells and in cells overexpressing Crn1p, suggest that Crn1p may provide a functional link between the actin and microtubule cytoskeletons in yeast.

Key words: actin • microtubule • coronin • cytoskeleton • yeast

G ROWING evidence suggests that the actin and microtubule cytoskeletons function interdependently during a number of cellular processes, including cleavage furrow positioning, neuronal growth cone steering, organelle transport, and nuclear migration (Gavin, 1997). In the budding yeast *Saccharomyces cerevisiae*, genetic evidence suggests that actin filaments and microtubules may function together during nuclear migration in mitotically dividing and mating cells (Palmer et al., 1992; Read et al., 1992). Nuclear and cytoplasmic microtubules in yeast emanate from spindle pole bodies, the yeast microtubule organizing centers. Before mitosis, the nucleus rotates and migrates to a position near the bud neck. These nuclear movements depend on cytoplasmic microtubules making transient attachments to the cell cortex (reviewed in Stearns, 1997). Although the molecular identities of the

cortical attachment sites are unknown, genetic and microscopy studies have led investigators to hypothesize that there may be multiple, functionally overlapping classes of attachment sites (Shaw et al., 1997). Based on genetic data and their cellular locations, cortical actin patches are candidates for microtubule attachment sites.

In budding yeast, the actin cytoskeleton is composed of two classes of filamentous structures, cortical actin patches and cytoplasmic actin cables (reviewed in Botstein et al., 1997). Throughout the mitotic cell cycle, the yeast actin cytoskeleton is in a constant state of remodeling. These dynamic changes in actin organization are regulated in part by actin-associated proteins, which modulate the nucleation, assembly, stabilization, cross-linking, and severing/depolymerization of actin filaments (Pollard, 1993; Ayscough, 1998).

We have isolated a novel component of the yeast cortical actin cytoskeleton, Crn1p (coronin1p), which shares strong sequence homology with the conserved actin binding protein coronin. Crn1p also contains an insert with two sequences (not found in other coronins) that share homol-

ogy with the microtubule binding region of MAP1B (Noble et al., 1989). Coronin was first identified as an actin-associated protein in *Dictyostelium discoideum*, where upon cell activation, it translocates to the cortical actin cytoskeleton at crown-shaped cell surface projections (de Hostos et al., 1991; Gerisch et al., 1995). Deletion of the coronin gene in *D. discoideum* leads to defects in cell migration, cytokinesis, phagocytosis, and fluid phase endocytosis (de Hostos et al., 1993; Maniak et al., 1995; Hacker et al., 1997). More recently, homologues of coronin have been identified in *C. elegans*, sea urchin, and bovine tissues (Suzuki et al., 1995; Zaphiropoulos and Toftgard, 1996; Terasaki et al., 1997), and a family of coronin genes has been identified in both mice and humans (Okumura et al., 1998). Whereas some coronin isoforms are expressed ubiquitously, others show tissue-specific patterns of expression. Coronin also was localized recently to the actin filament tails of *Listeria monocytogenes* in infected mammalian cells (David et al., 1998). This localization, as well as the localization of coronin to sites of dynamic actin assembly in migrating *D. discoideum* cells, suggests that coronin may be involved in regulating actin assembly. However, until now, the biochemical activities of coronin have been unknown.

Here, we demonstrate that Crn1p promotes the rapid barbed-end assembly of actin filaments and cross-links them into bundles and networks. We also show that Crn1p binds to microtubules in vitro via its unique region and is capable of cross-linking actin filaments and microtubules. These activities, supported by genetic data presented here, raise the possibility that Crn1p may link functions of the actin and microtubule cytoskeletons in yeast.

Materials and Methods

Strains and Growth Conditions

Yeast were grown using standard procedures and media as described in Guthrie and Fink (1990). The yeast strains used in this study are listed in Table I.

Purification of Tubulin and Actin

Bovine brain tubulin was purified as described in Mitchison and Kirschner (1984) by assembly and disassembly cycling. Tubulin was further purified by phosphocellulose and DEAE chromatography. Tubulin was eluted from the DEAE column with a linear salt gradient (0.1–0.6 M NaCl). Tubulin-containing fractions were pooled, desalted and concentrated at 4°C to 80 μM in PME buffer (80 mM KOH-Pipes [pH 6.8], 1 mM MgCl$_2$, 1 mM EGTA) supplemented with 1 mM GTP using Centriprep 10 devices (Amicon). Tubulin was frozen in aliquots in liquid N$_2$ and stored at −80°C. Yeast tubulin was purified and stored as described previously (Barnes et al., 1992).

Yeast actin was purified by affinity chromatography using immobilized DNase I and formamide as an eluant (Zechel, 1980). Fresh, commercially available yeast (Red Star Yeast) were washed once in 2 vol of H$_2$O, resuspended in 0.2 vol of H$_2$O, frozen in liquid N$_2$ as 200–400-μl drops and stored at −80°C. To lyse cells, ∼40–100 g of frozen yeast were transferred to a stainless steel Waring blender (1 liter), to which liquid nitrogen was added to just cover the yeast. The frozen yeast were blended for 20–30 s on high speed, until all of the liquid nitrogen evaporated from the chamber. More liquid nitrogen was added to the blender to cover the yeast powder, and the blending cycle was repeated four more times. The lysed yeast cells can be stored as a frozen powder at −80°C for months without detectable degradation.

A DNase I affinity column was constructed by coupling 200 mg of DNase I (Boehringer) to 20 ml of Affigel-10 (BioRad). The DNase I coupled resin was loaded into a 2.5-cm-diam column (BioRad) and washed with 5 column volumes of G-buffer (10 mM Tris [pH 7.5], 0.2 mM CaCl$_2$, 0.2 mM DTT, 0.2 mM ATP). To prepare a yeast high speed supernatant (HSS), ∼250 g of frozen, lysed yeast powder was mixed at a 1:1 ratio (wt/vol) with G-buffer supplemented with 1 mM DTT and protease inhibitors (1 mM phenylmethylsulfonyl fluoride [PMSF] and 1 μg/ml each of anti-pain, leupeptin, pepstatin A, chymostatin, and aprotinin). The mixture was stirred continuously with a spatula at room temperature until all of the visible ice chunks were thawed. While still cold, the mixture was centrifuged at 45,000 rpm for 2 h in a Beckman 45Ti rotor at 4°C. The supernatant was carefully removed by pipetting, and was filtered through six layers of cheesecloth into a beaker on ice. The HSS (∼200 ml) was loaded onto a DNase I affinity column at a flow rate of 2 ml/min. The column was washed sequentially with 40 ml of G-buffer, 40 ml of G-buffer plus 0.2 M NH$_4$Cl, 40 ml of G-buffer plus 10% deionized formamide, and 40 ml of G-buffer. The actin was eluted from the column with 40 ml of G-buffer plus 50% deionized formamide. (NH$_4$)$_2$SO$_4$ was added to 0.35 g/ml and dissolved by gentle mixing. The actin was precipitated by overnight incubation on ice, followed by centrifugation for 10 min at 12,000 g, 4°C. The pellet was resuspended in 5 ml of G-buffer and dialyzed twice, 4 h each, against 1 liter of G-buffer. The yeast actin was precleared in a microfuge for 5 min at 4°C, concentrated at 4°C to 40–70 μM in Centricon 10 devices, frozen in aliquots in liquid N$_2$, and stored at −80°C.

Isolation of S. cerevisiae Proteins on a Microtubule Affinity Column

Microtubule affinity columns were constructed using taxol-stabilized bovine microtubules as described (Miller et al., 1991; Barnes et al., 1992).

Table I. Yeast Strains Used in this Study

Name	Genotype
DDY130	*MAT*a *his3-Δ200, leu2-3,112, ura3-52, lys2-801am*, GAL$^+$
DDY903	*MAT**a** his3-Δ200, leu2-3,112, ura3-52, lys2-801am*
DDY1088	*MAT**a** ade2-101, ade3-130, leu2-3,112, ura3-52*
DDY1089	*MAT*α *ade2-101, ade3-130, leu2-3,112, ura3-52, lys2-801am*
DDY1090	*MAT**a**/MAT*α *ade2-101/ade2-101, ade3-130/ade3-130, leu2-3,112/leu2-3,112, ura3-52/ura3-52, lys2-801am/LYS2*
DDY1518	*MAT*α *his3-Δ200, leu2-3,112, ura3-52, lys2-801am, ade2-101, trp1-Δ99, can1-1, crn1Δ::LEU2*
DDY1519	*MAT*α *his3-Δ200, leu2-3,112, ura3-52, lys2-801am, ade2-101, trp1-Δ99, can1-1*
DDY322	*MAT*α *his3-Δ200, leu2-3, 112, ura3-52, abp1Δ::HIS3*
DDY1520	*MAT**a** his3-Δ200, leu2-3,112, ura3-52, trp1-Δ99, aip1Δ::HIS3*
DDY582	*MAT**a** ade2-101, his3-Δ200, leu2-3,112, ura3-52, trp1-Δ99, cap2-Δ1::HIS3*
DDY1266	*MAT*α *ade2-101, his3-Δ200, leu2-3,112, ura3-52, trp1-Δ99, rho$^+$, cof1-22*::HIS3
DDY1438	*MAT*α *his3-Δ200, leu2-3,112, ura3-52, lys2-801am, las17Δ::HIS3*
DDY1024	*MAT**a** his3-Δ200, leu2-3,112, ura3-52, lys2-801am, ade2-101, ade3-130, pfy1-116::HIS3*
DDY318	*MAT*α *his3-Δ200, leu2-3,112, ura3-52, lys2-801am*, GAL$^+$, *sac6Δ::HIS3*
DDY949	*MAT**a** his3-Δ200, leu2-3,112, ura3-52, trp1-Δ99, rvs167Δ::TRP1*
DDY1434	*MAT**a** ade2-101, his3-Δ200, leu2-3,112, ura3-52, twf1Δ::HIS3*
DDY1492	*MAT*α *ade4, his3-Δ200, leu2-3,112, ura3-52, tub2-201, act1-159::HIS3*

Yeast extracts were prepared as follows: yeast were grown in YPD to an optical density of 1 at 600 nm, washed once in 2 vol of H$_2$O, resuspended in 0.2 vol of H$_2$O, frozen in liquid nitrogen as 200–400-μl drops, and stored at $-80°$C. The frozen yeast were lysed as described above. A HSS was prepared for the microtubule affinity column by mixing frozen lysed yeast powder at a 1:1 ratio (wt/vol) with room temperature buffer C (50 mM KOH-Hepes [pH 7.5], 50 mM KCl, 2 mM MgCl$_2$, and 1 mM EDTA), supplemented with 1 mM DTT and protease inhibitors (as above). The thawed mixture was centrifuged at 40,000 rpm for 60 min in a Beckman type 40 rotor at 4°C. The supernatant was removed by pipetting and filtered through six layers of cheesecloth. Then, 10% glycerol (vol/vol) was added to the HSS to stabilize proteins as described in Miller et al. (1991).

At a flow rate of 2 ml/h, 20 ml of the HSS and glycerol was loaded onto either a 1-ml microtubule or BSA control column ($\sim$1 mg/ml protein attached to a 1:1 mixture of Affigel 10 [BioRad] and CL6B sepharose [Pharmacia Biotech, Piscataway, NJ]) at 4°C. The columns were washed with 40 ml buffer CX (buffer C, supplemented with 1 mM DTT, protease inhibitors and 10% glycerol [vol/vol]). Proteins were eluted from the columns by sequential washes of 10 ml buffer CX plus 1 mM ATP and 1 mM GTP, 0.1 M KCl and 0.5 M KCl, collecting 1-ml fractions. Half of each fraction was TCA precipitated (Sambrook et al., 1989) and analyzed by SDS-PAGE and Coomassie blue staining to identify microtubule column-specific proteins. The remaining half of the relevant fractions were desalted and concentrated in Centricon 10 devices. Samples were digested with trypsin. The resulting peptides were analyzed by LC/MS/MS tandem mass spectrometry and matched to proteins in the *Saccharomyces cerevisiae* genome database as described in McCormack et al. (1997).

Plasmid Construction and Deletion of the CRN1 Gene

The coding region of *CRN1* (YLR429w) was amplified from S288C yeast genomic DNA using the Expand PCR kit from Boehringer with 5′ and 3′ primers (GATGCGGCCGCCTCTTGACCAAATACGATGATTCT-TCC and AGAGAATCCGATTAAAATGATTCTTCAGCCATGTG-GCCG, respectively). The PCR products were digested with NotI and BamHI and ligated into the NotI and BamHI sites of the Bluescript KS+ vector (Stratagene). The resulting plasmid is referred to as pBS-CRN1. pcrn1Δ::LEU2 was generated by replacing the 1,156-bp MscI-BglII fragment of pBS-CRN1 with a 2,220–bp HindIII-BamHI *LEU2* gene fragment. To construct GST-CRN1 fusion plasmids for expression in bacteria, DNA sequences encoding amino acids 1–651, 1–599, 1–400, and 400–651 of yeast coronin were amplified from pBS-CRN1 by PCR using primers that generate BamHI and NsiI sites at the 5′ and 3′ ends, respectively. The PCR products were ligated into BamHI-NsiI digested pGAT2 vector (a GST-fusion derivative of pBAT; Peränen et al., 1996) to generate pGAT2-CRN(1–651), pGAT2-CRN(1–599), pGAT2-CRN(1–400), and pGAT2-CRN(400–651). To construct a GFP-CRN1 fusion plasmid, the coding sequence of *CRN1* was amplified from pBS-CRN1 by PCR using primers that generate BamHI and XbaI sites at the 5′ and 3′ ends, respectively. The PCR product was ligated into BamHI-XbaI cut pTS408 (Carminati and Stearns, 1997) to generate a CEN plasmid with a GFP-CRN1 fusion gene under control of the *GAL10* promoter. To construct a GST-CRN1 fusion for expression in yeast, the BamHI-XbaI insert described above was ligated into BamHI-XbaI digested pEGKT vector (Mitchell et al., 1993) to generate pEGKT-CRN1. All PCR-generated insertions were sequenced to insure that mutations were not introduced into the *CRN1* sequences.

To generate disruptions of the *CRN1* gene, pcrn1Δ::LEU2 was linearized and used to transform the diploid strain DDY1090. Leu$^+$ transformants were isolated on selective medium and deletion of the *CRN1* gene was verified by PCR with primers to sequences in *LEU2* and outside of the *CRN1* coding region. Hemizygotes were sporulated and the resulting tetrads dissected. Tetrad progeny showed a 2:2 segregation of the *LEU2* marker. Loss of *CRN1* gene expression in Leu$^+$ haploids was verified by immunoblotting with Crn1p antibodies.

Recombinant Crn1p Expression and Purification

Full-length and partial coding sequences of *CRN1* were expressed as glutathione-*S*-transferase (GST)[1] fusion proteins in *E. coli* BL21 (DE3) cells

---

1. *Abbreviations used in this paper:* GFP, green fluorescent protein; GST, glutathione-*S*-transferase; HSS, high speed supernatant; IPTG, isopropyl-thio-β-D-galactoside.

as described (Peränen et al., 1996). Cells transformed with pGAT2-CRN(1–651), pGAT2-CRN(1–599), pGAT2-CRN(1–400), and pGAT2-CRN(400-651) were grown in 2,000 ml of LB medium + 100 μg/ml ampicillin at 37°C. At an optical density of 0.5 at 600 nm, expression was induced by the addition of 0.4 mM isopropyl-thio-β-D-galactoside (IPTG). After 4 h, cells were pelleted, washed with 40 ml PBS, resuspended in 30 ml PBS plus 1 mM PMSF and lysed by sonication. The lysate was centrifuged at 10,000 rpm for 10 min at 4°C in an SA600 rotor (Sorvall/DuPont). The GST fusion proteins were purified from the supernatants using glutathione-agarose beads (0.5 ml). The glutathione agarose-bound GST-Crn1p fusion proteins were incubated overnight in 1 ml PBS containing 0.02 mg/ml thrombin to release coronin into the supernatant. To remove the thrombin, the supernatant was mixed with 50 μl of thrombin-binding *p*-aminobenzamidine-agarose (Sigma Chemical Co.) and tumbled for 30 min at 4°C. The beads were pelleted to remove thrombin, and the supernatant was loaded directly onto a 5/5 mono Q column (Pharmacia) equilibrated in buffer B (20 mM KOH-Hepes [pH 7.5], 50 mM KCl). The column was washed with 10 ml buffer B and the proteins were eluted using a linear salt gradient (0.1–0.5 M KCl). Crn1p-containing fractions were identified by SDS-PAGE and Coomassie blue staining. The desired fractions were pooled, concentrated to 20–30 μM, desalted at 4°C in a Centricon 10 device, frozen in aliquots in liquid N$_2$ and stored at $-80°$C.

Generation of Anti-Crn1p Antibodies and Immunoblotting

Three mice were immunized with recombinant full-length Crn1p to produce polyclonal ascites antibodies. On days 1, 8, and 20, each mouse received 25–50 μg of Crn1p diluted in PBS to 100 μl and mixed 1:1 with RIBI (Ribi ImmunoChem). On day 27, tailbleed immunoreactivity (1:500 dilution) was tested on immunoblots of total wild-type and *crn1Δ* cell proteins. Two mice sera recognized Crn1p, and these mice were immunized again on day 28. On day 33, the mice were injected subcutaneously with sarcoma cells to induce the formation of ascites fluid, which was tapped on day 45. The ascites fluid ($\sim$10 ml from each mouse) was centrifuged for 5 min at 13,000 rpm in a microfuge and the supernatant frozen in 1-ml aliquots in liquid N$_2$ and stored at $-80°$C. Antibodies were used at 1:1,000 dilution on immunoblots and 1:100 dilution for immunofluorescence. Immunoblotting was performed by standard methods (Sambrook et al., 1989) using 1:1,000 dilutions of antibodies that recognize Crn1p and yeast actin.

Actin Filament and Microtubule Cosedimentation Assays

For actin filament cosedimentation assays, filaments were assembled from purified yeast actin in G-buffer by the addition of 0.1-vol of 10× Initiation Mix (IM) buffer: (20 mM MgCl$_2$, 0.5 M KCl, 5 mM ATP) and incubated for 30 min at 25°C. For microtubule cosedimentation assays, purified bovine brain tubulin was assembled in 30% glycerol and 1 mM GTP for 30 min at 35° C, then stabilized by addition of 20 μM taxol. Microtubules dilutions were made in buffer C supplemented with 10 μM taxol and 1 mM GTP. F-actin and microtubule cosedimentation assays both were performed using 40-μl reactions, containing variable concentrations of Crn1p fragments and actin filaments or microtubules. The reactions were incubated for 20 min at 25°C, and then centrifuged for 30 min at 25°C, 90,000 rpm in a TLA100 rotor (Beckman). Equal portions of the pellets and supernatants were analyzed by SDS-PAGE and Coomassie staining or immunoblotting with Crn1p antibodies. For determining the dissociation constant (K_d) of the Crn1p:F-actin binding interaction, 10 μM phalloidin was added to the reaction buffers to stabilize the actin filaments.

Actin Filament Bundling Assays

Three assays were used to test the effects of Crn1p on actin filament bundling: low speed pelleting assay, falling ball assay to measure apparent viscosity, and visualization of filaments by electron microscopy. For low speed pelleting assays, various concentrations of Crn1p were added to preassembled yeast actin filaments (2 μM) and incubated for 15 min at 25°C. The reactions were centrifuged at low speed (13,000 g) for 3 min, and the supernatants and pellets were analyzed by SDS-PAGE and Coomassie staining. Actin filaments remain in the supernatant under these centrifugation conditions, whereas F-actin bundles pellet. The falling ball assay was used to measure apparent viscosity (Pollard and Cooper, 1982). These assays were performed using actin filaments at steady state. In one set of reactions (see Fig. 3), variable concentrations of Crn1p were added

to preassembled F-actin (7 μM final concentration), and, after incubation at 25°C for 30 min, viscosity was measured. In a different set of reactions (see Fig. 4), variable concentrations of Crn1p were copolymerized with monomeric actin (7 μM) for 30 min at 25°C, and then viscosity was measured. Aliquots from both sets of reactions were removed and spotted onto copper grids freshly coated with formvar, negatively stained with 1% aqueous uranyl acetate, and examined using a transmission electron microscope.

Actin Filament Assembly and Disassembly Assays

For light scattering assays, purified yeast actin (50 μM) in G-buffer was thawed overnight at 4°C and precleared by centrifugation for 60 min at 4°C, 90,000 rpm in a TLA100 rotor. Then, 80 μl of monomeric actin (6.25 μM) was added to 10 μl of 10× IM buffer and 10 μl of Crn1p or buffer. The reactions contained a final concentration of 5 μM G-actin and 0, 0.1, or 0.5 μM Crn1p. The reaction was mixed by pipetting and immediately transferred to a quartz fluorometer cuvette with 3-mm light path (Helma), marking time 0. Actin filament assembly was monitored by increase in light scattering at 400 nm in a F-4010 fluorescence spectrophotometer (Hitachi) at 25°C. To prevent bubble formation, all solutions were brought to room temperature before use in the assay. To reduce noise in the spectra, solutions were precleared immediately before use by centrifugation for 5 min, 13,000 g. Steady state assembly of actin was reached by 20–25 min in all reactions, as determined by light scattering and measurement of polymer mass. To measure polymer mass, samples at time points were centrifuged for 30 min at 25°C, 90,000 rpm in a TLA100 rotor and the actin levels in the supernatants and pellets were determined by SDS-PAGE and Coomassie staining.

For pyrene-actin assembly assays, variable concentrations of Crn1p were added to 5 μM monomeric actin (4 μM yeast actin + 1 μM pyrene-labeled rabbit muscle actin; Cytoskeleton) and assembly initiation salts at time 0. Assembly was monitored by change in pyrene fluorescence at excitation 365 nm, emission 407 nm in a fluorometer. For F-actin disassembly assays, different concentrations of Crn1p, Sac6p or cytochalasin D were added to 5 μM preassembled actin filaments (4 μM yeast actin and 1 μM pyrene-labeled rabbit muscle actin) and incubated for 15 min at 25°C. Filament disassembly was initiated at time 0 by the addition of 40 μM latrunculin A (an actin monomer sequestering agent), and disassembly was monitored by change in pyrene fluorescence as above.

Determination of Actin Critical Concentration

To measure the effects of Crn1p on actin Cc, three different concentrations of purified yeast actin filaments (0.5, 1, or 2 μM) were mixed with Crn1p at four different stoichiometries of Crn1p:actin (0:1, 1:10, 1:3, or 1:1). After incubation at 25°C, the actin filaments were pelleted by centrifugation for 30 min at 90,000 rpm, 25°C in a TLA100 rotor. The levels of actin in the supernatants were determined by SDS-PAGE and Coomassie staining.

Light Microscopy

Cells were prepared for immunofluorescence microscopy as described in Ayscough and Drubin (1997). To disrupt the actin cytoskeleton, log-phase yeast cultures were treated with 400 μM latrunculin A for 5 min before chemical fixation (Ayscough et al., 1997). The localization of a green fluorescent protein (GFP)-Crn1p fusion protein under the expression of the GAL10 promoter was examined in living yeast cells. Cells transformed with pGFP-CRN1 were grown in synthetic selective media plus glucose to log-phase (OD₆₀₀ 0.2), washed once and transferred to synthetic selective media plus 2% galactose. After 12 h of growth at 25°C, cells were mounted on slides and examined by fluorescence microscopy. Fluid-phase endocytosis in wild-type (DDY1088) and crn1Δ cells (DDY1521) was assayed by uptake of the fluorescent dye lucifer yellow as described (Dulic et al., 1991). Overexpression of GST-Crn1p was induced from the 2μ plasmid pEGKT-CRN1, marked with both URA3 and leu2-d. To achieve a high number of plasmids, wild-type cells (DDY130) transformed with pEGKT-CRN1 were grown in minimal media lacking uracil and leucine. Induction of expression from the GAL10 promoter was achieved as described above.

Results

Isolation of Actin and the YLR429w Gene Product by Microtubule Affinity Chromatography

In a previous report, we used LC/MS/MS tandem mass spectrometry to identify S. cerevisiae proteins purified from yeast extracts by cosedimentation with microtubules (McCormack et al., 1997). Here, we used similar analyses and identified two proteins of 48 and 85 kD that were isolated from S. cerevisiae extracts by microtubule affinity chromatography. A fraction eluted from the microtubule column by 0.5 M KCl contains three prominent bands of apparent molecular masses 48, 55, and 85 kD (Fig. 1 A). Different proteins, which are not shown, were eluted by 0.1 M KCl before the 0.5 M KCl elution. All of the peptides identified in this sample are listed in Fig. 1 A and were derived from either actin or the YLR429w gene product. Subsequent immunoblotting verified that the 48-kD band is yeast actin, the 55-kD band is bovine tubulin, which leaches off the column in high salt washes, and the 85-kD protein is the product of the YLR429w gene. Bovine tubulin peptides were not identified by the mass spectrometry analysis because they are not present in the S. cerevisiae genome database.

The YLR429w Gene Product Shares Sequence Homology with an Actin Binding Protein and a Microtubule-associated Protein

The YLR429w gene is predicted to encode a 651–amino acid protein (Fig. 1 B) with a mass of 72.5 kD. BLAST searches (Pearson and Lipman, 1988) revealed that YLR429w is homologous to members of the coronin family of actin-binding proteins from Caenorhabditis elegans, Dictyostelium discoideum, Bos taurus, and Homo sapiens (deHostos et al., 1991; Suzuki et al., 1995; Zaphiropoulos and Toftgard, 1996). The YLR429w gene, which was named CRN1 (coronin1), does not show strong homology to any other genes in the S. cerevisiae database. Alignment of the primary sequences of coronins from different species showed that they are highly conserved and have similar domain structures (Fig. 1 C). The regions shaded in Fig. 1 C share ~45% amino acid identity. The NH₂ terminus (amino acids 1–400 in Crn1p) contains five WD-repeats, structural motifs found in proteins of diverse function and which form a β–propeller-like conformation in the β subunit of heterotrimeric G proteins (Neer et al., 1994; Wall et al., 1995). The COOH termini (last 50 amino acids) of all known coronins are strongly predicted (a probability of 1 on Prosite) to form α-helical coiled coil structures.

Each coronin also contains a unique region that varies greatly in length and is distinct in sequence. The unique region of Crn1p (boxed in Fig. 1 B) shares no significant sequence homology with the unique regions of other coronins. However, two sequences in the Crn1p unique region (amino acids 408–466 and 535–568; underlined in Fig. 1 B) share 32/53% and 33/58% amino acid sequence identity/similarity, respectively, with a sequence in mammalian microtubule-associated protein MAP1B (amino acids 646–732) that has been shown to be sufficient for microtubule binding in vitro and in vivo (Noble et al., 1989). Fig. 1 D shows a sequence alignment between a segment of the MAP1B
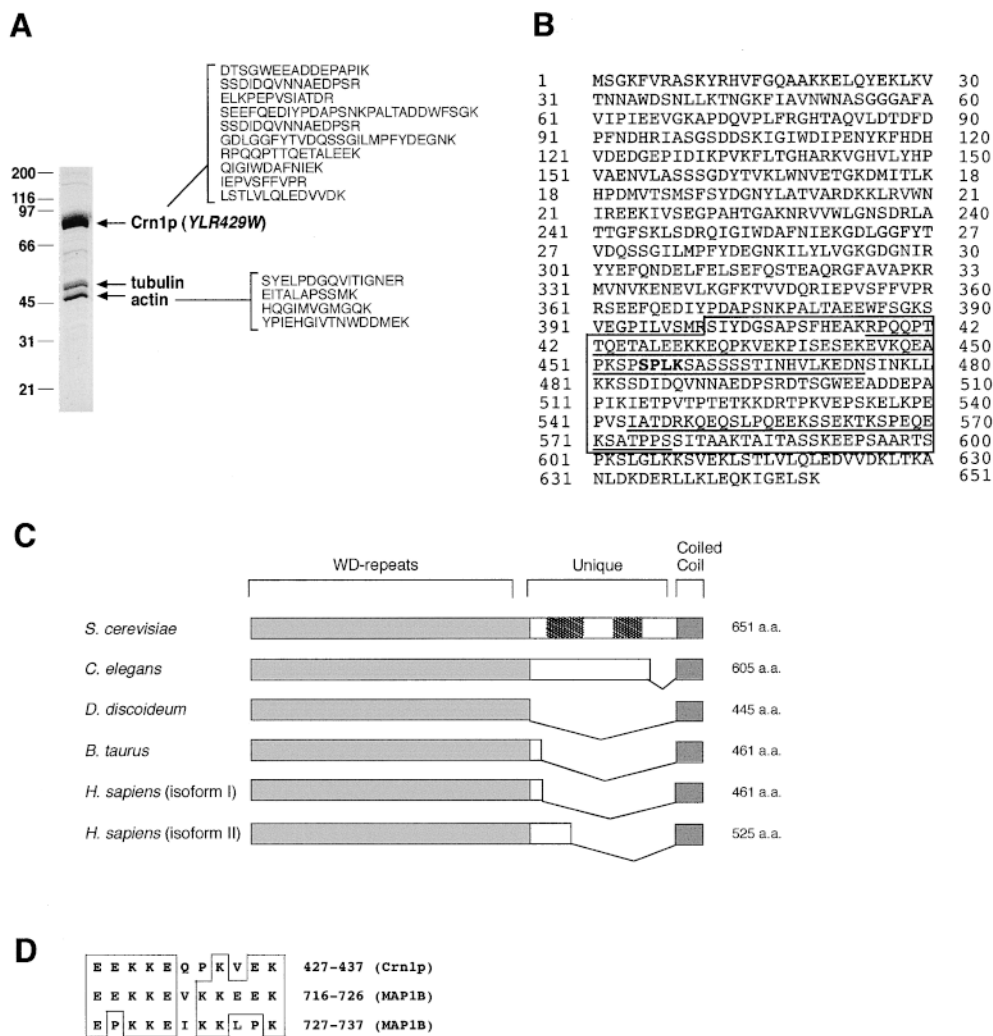
A

DTSGWEEADDEPAPIK
SSDIDQVNNAEDPSR
ELKPEPVSIATDR
SEEFQEDIYPDAPSNKPALTADDWFSGK
SSDIDQVNNAEDPSR
GDLGGFYTVDQSSGILMPFYDEGNK
RPQQPTTQETALEEK
QIGIWDAFNIEK
IEPVSFFVPR
LSTLVLQLEDVVDK

200 —
116 —
97 —
66 —
→ Crn1p (*YLR429W*)

45 — → tubulin
→ actin

SYELPDGQVITIGNER
EITALAPSSMK
HQGIMVGMGQK
YPIEHGIVTNWDDMEK

31 —
21 —

B

1	MSGKFVRASKYRHVFGQAAKKELQYEKLKV	30
31	TNNAWDSNLLKTNGKFIAVNWNASGGGAFA	60
61	VIPIEEVGKAPDQVPLFRGHTAQVLDTDFD	90
91	PFNDHRIASGSDDSKIGIWDIPENYKFHDH	120
121	VDEDGEPIDIKPVKFLTGHARKVGHVLYHP	150
151	VAENVLASSSGDYTVKLWNVETGKDMITLK	18
18	HPDMVTSMSFSYDGNYLATVARDKKLRVWN	21
21	IREEKIVSEGPAHTGAKNRVVWLGNSDRLA	240
241	TTGFSKLSDRQIGIWDAFNIEKGDLGGFYT	27
27	VDQSSGILMPFYDEGNKILYLVGKGDGNIR	30
301	YYEFQNDELFELSEFQSTEAQRGFAVAPKR	33
331	MVNVKENEVLKGFKTVVDQRIEPVSFFVPR	360
361	RSEEFQEDIYPDAPSNKPALTAEEWFSGKS	390
391	VEGPILVSMRSIYDGSAPSFHEAKRPQQPT	42
42	TQETALEEKKEQPKVEKPISESEKEVKQEA	450
451	PKSPSPLKSASSSSTINHVLKEDNSINKLL	480
481	KKSSDIDQVNNAEDPSRDTSGWEEADDEPA	510
511	PIKIETPVTPTETKKDRTPKVEPSKELKPE	540
541	PVSIATDRKQEQSLPQEEKSSEKTKSPEQE	570
571	KSATPPSSITAAKTAITASSKEEPSAARTS	600
601	PKSLGLKKSVEKLSTLVLQLEDVVDKLTKA	630
631	NLDKDERLLKLEQKIGELSK	651

C

D

EEKKEQPKVEK 427–437 (Crn1p)
EEKKEVKKEEK 716–726 (MAP1B)
EPKKEIKKLPK 727–737 (MAP1B)

Figure 1. (A) Coisolation from yeast extracts of actin and Crn1p on a microtubule affinity column. Proteins were isolated from *S. cerevisiae* extracts using an affinity column containing taxol-stabilized bovine microtubules (see Materials and Methods). Shown is a Coomassie-stained gel of proteins eluted from the column by 0.5 M KCl. The proteins in this fraction were digested with trypsin, and the resulting peptides were identified by LC/MS/MS tandem mass spectrometry and matched to predicted gene products in the *S. cerevisiae* genome database. All of the yeast peptides identified in the column fraction shown were derived from actin or the product of the *YLR429w* gene. The peptide sequences are shown adjacent to the protein bands from which they were derived. (B) Predicted amino acid sequence of the *YLR429w* (*CRN1*) gene product. The unique region is boxed, and contains two sequences (underlined) that share homology with the microtubule binding region of MAP1B. A single consensus target sequence for Cdc28p kinase is shown in bold. (C) Alignment of the domain structures of *S. cerevisiae*, *C. elegans*, *D. discoideum*, *B. taurus*, and *H. sapiens* coronins. Each protein contains a conserved WD repeat region and COOH-terminal coiled-coil domain (shaded regions). In addition, each coronin has a COOH-terminal unique region (not shaded). The unique regions vary greatly in length and sequence. The unique region of yeast coronin (*CRN1*) is distinct from other coronins and contains two sequences (hatched boxes) with homology to the microtubule binding region of MAP1B. (D) Alignment of a sequence in MAP1B that contains a KKE/D microtubule binding motif with a similar sequence found in the unique region of *S. cerevisiae* coronin (Crn1p).

microtubule binding region that contains a KKE/D microtubule binding motif and a short sequence in the Crn1p unique region.

The Abundance of Crn1p in Yeast Cells

Full-length Crn1p was expressed in *E. coli* and purified as described (see Materials and Methods). The resulting protein is soluble and has an apparent molecular mass of 85 kD on SDS-PAGE gels, similar to that of Crn1p identified on immunoblots of yeast extracts. Antibodies were generated against Crn1p. The immunoreactivity of the antibodies is highly specific on immunoblots (Fig. 2 A). To estimate the abundance of Crn1p in yeast cells, total proteins from an asynchronously dividing culture of wild-type yeast (DDY1090) were immunoblotted in parallel with known amounts of purified yeast actin and Crn1p. The blots were probed with actin and Crn1p antibodies and the signals from yeast extracts and purified proteins were compared (not shown). Consistent with previous reports, actin comprised ~0.1% of total cellular protein (Karpova et al., 1995). Crn1p comprised ~0.01% of total cellular protein. Thus, Crn1p is ~10-fold less abundant than actin, and is similar in abundance to capping protein and cofilin in yeast (Karpova et al., 1995; P. Lappalainen, unpublished results).

Crn1p Binds to Actin Filaments and Microtubules In Vitro

Previous studies have shown that coronin from *Dictyostelium discoideum* and *Bos taurus* binds directly to actin filaments in vitro (de Hostos et al., 1991; Suzuki et al., 1995). First, we tested whether yeast coronin (Crn1p) binds to ac-
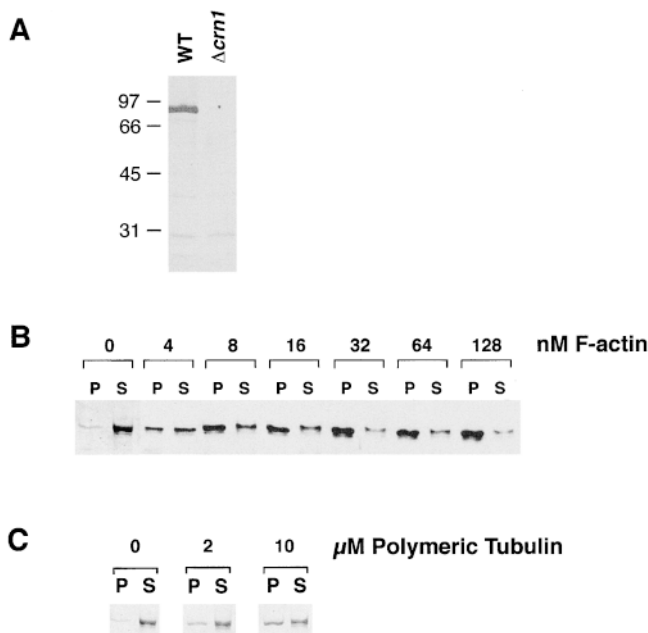
A

WT Δcrn1

97 —
66 —

45 —

31 —

B

0   4   8   16   32   64   128   nM F-actin

P S P S P S P S P S P S P S

C

0   2   10   *μM Polymeric Tubulin*

P S P S P S

Figure 2. Crn1p binds to actin filaments and microtubules. (A) Immunoblot of total wild-type (WT) and *crn1Δ* cell proteins probed with coronin antibodies. (B) Crn1p binds to actin filaments with high affinity. Crn1p (0.5 nM) was mixed with variable concentrations of phalloidin-stabilized yeast actin filaments. After incubation, the actin filaments were pelleted, and the pellets and supernatants were analyzed by SDS-PAGE and immunoblotting with Crn1p antibodies. (C) Crn1p binds to microtubules with weak affinity. Full-length Crn1p (0.5 μM) was mixed with variable concentrations of taxol-stabilized bovine brain microtubules. After incubation, the microtubules were pelleted, and the pellets (P) and supernatants (S) were analyzed by SDS-PAGE and Coomassie staining.

tin filaments in vitro. Initial cosedimentation assays with purified Crn1p and yeast actin filaments showed that Crn1p binds with high affinity to F-actin (K_d below 0.2 μM). The specificity of the interaction was demonstrated by the ability of excess recombinant Crn1p to compete with radio-labeled in vitro translated Crn1p for F-actin binding (not shown). To measure the strength of the Crn1p–F-actin binding interaction, it was necessary to reduce the Crn1p and F-actin concentrations in the reactions to nanomolar levels. Because F-actin disassembles under these conditions (the critical concentration of yeast actin is 0.1–0.2 μM), 10 μM phalloidin was added to stabilize the actin filaments. A constant concentration of Crn1p (0.5 nM) was added to variable concentrations of phalloidin-stabilized yeast actin filaments (0, 4, 8, 16, 32, 64, and 128 nM) in a cosedimentation assay. To control for nonspecific interactions that could occur at such low concentrations of actin filaments and Crn1p, 0.1 mg/ml BSA was included in these reactions. The pellets and supernatants were immunoblotted and probed with Crn1p antibodies (Fig. 2 B). At F-actin concentrations of 4×10^{-9} M and 8×10^{-9} M, ~40 and 60% of the Crn1p bound to F-actin, respectively. At higher concentrations, >80% of the Crn1p bound to F-actin. From these data, we estimate that the apparent dissociation constant (K_d) of the interaction is ~6×10^{-9} M

(6 nM), which indicates a very strong interaction in comparison to other characterized actin binding proteins (Pollard, 1993). To determine the stoichiometry of binding at saturation, we used a constant concentration of actin filaments (1 μM) and variable concentrations of Crn1p (0.125, 0.25, 0.5, 1, 2, and 4 μM) in a cosedimentation assay. F-actin binding saturated at a 1:1 molar ratio of Crn1p to F-actin (not shown).

To test the ability of Crn1p to bind to microtubules, variable concentrations of taxol-stabilized bovine microtubules were added to Crn1p (0.5 μM) in a cosedimentation assay (Fig. 2 C). Crn1p bound weakly to microtubules, but in a concentration-dependent manner, suggesting a specific binding interaction. Approximately 20% of the Crn1p bound at 2 μM microtubules, and ~40% bound at 10 μM microtubules, suggesting a modest K_d of 15–20 μM. Similar affinities were observed using yeast microtubules or in vitro translated Crn1p.

Crn1p Cross-links Actin Filaments into Bundles

Next, we tested the effects of Crn1p on actin filament cross-linking using a low speed pelleting assay (Sandrock et al., 1997). Neither F-actin nor Crn1p alone pelleted upon centrifugation at low speeds (15,000 *g*). However, the addition of Crn1p to preassembled actin filaments caused low speed pelleting of a Crn1p–F-actin complex (Fig. 3 A). This result suggests that Crn1p cross-links actin filaments, but does not reveal whether Crn1p forms actin bundles or more complex networks or gels. Therefore, we measured the effects of Crn1p on the apparent viscosity of actin solutions using the falling ball assay (Pollard and Cooper, 1982). In this assay, the formation of orthogonal networks or gels increases apparent viscosity, whereas the formation of F-actin bundles decreases apparent viscosity. As shown in Fig. 3 B, the addition of Crn1p to preassembled actin filaments led to a concentration-dependent decrease in apparent viscosity, suggesting the formation of F-actin bundles.

As a positive control for bundling, we measured the effects of Sac6p/fimbrin on apparent viscosity. As shown in Fig. 3 B, purified yeast Sac6p/fimbrin caused a concentration-dependent decrease in solution viscosity below concentrations of 0.7 μM Sac6p (~1 Sac6p to 10 actin molar stoichiometry). However, at higher concentrations/molar ratios of Sac6p to actin, the apparent viscosity increased. Examination of these reactions by electron microscopy revealed large aggregates of bundled F-actin that likely impaired the mobility of the falling ball in capillary tubes. Similarly, we observed discontinuous falling ball migration in reactions containing concentrations of Crn1p above 2.5 μM (5 and 10 μM). These data are not shown in Fig. 3 B because in these reactions the migration of the ball was highly sporadic (often stalling), thus making measurements unreliable. Electron microscopy revealed similar tangles of actin filament bundles at these high concentrations of Crn1p (not shown). Because Crn1p is present in yeast at a molar ratio of ~1 Crn1p per 10 actin subunits, 1:10 ratios in viscosity assays may be most relevant in vivo. A 1:10 ratio of either Crn1p or Sac6p to actin caused a decrease in viscosity and the formation of long actin filament bundles seen by electron microscopy (Fig. 3 C).
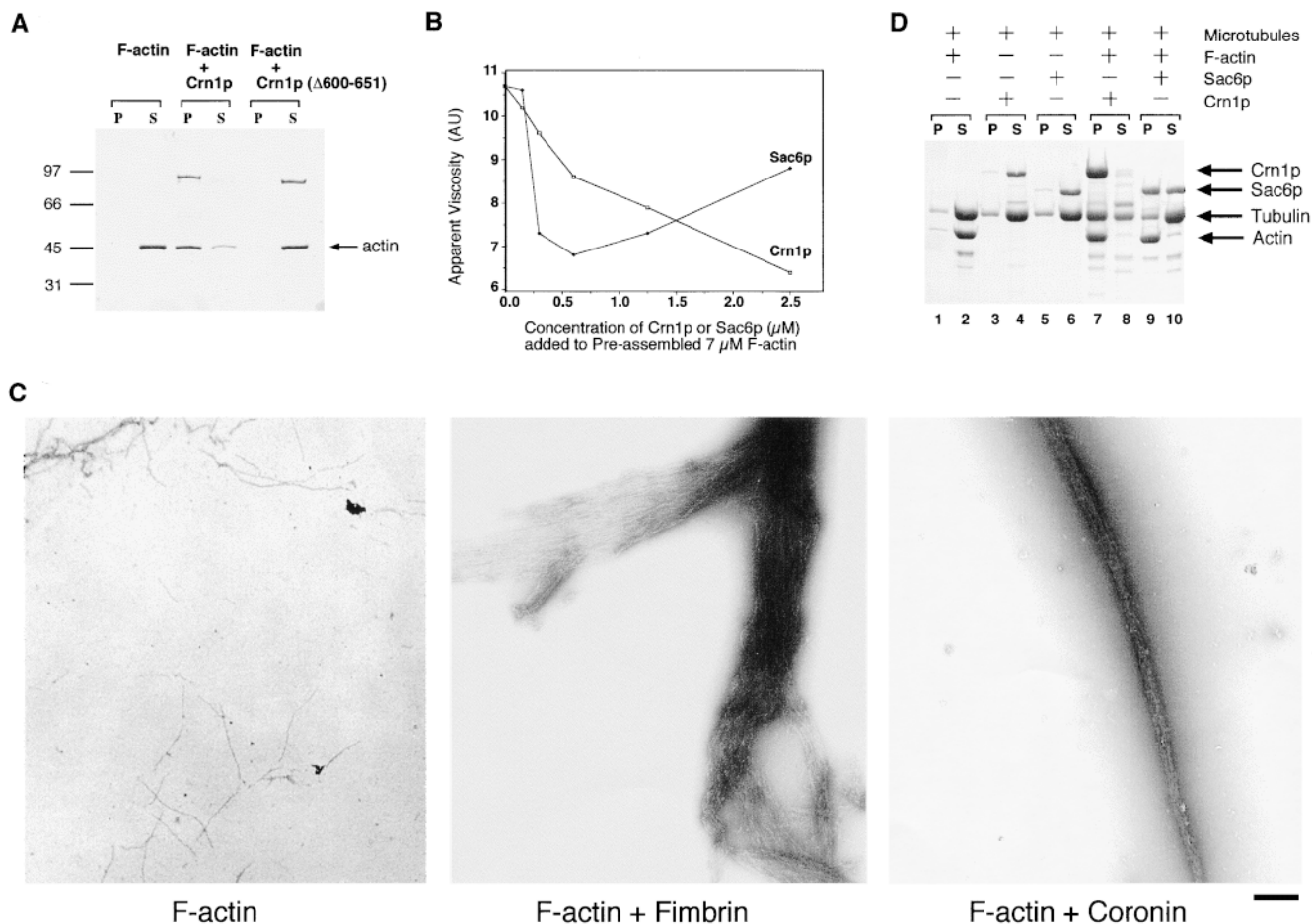
Figure 3. Crn1p bundles actin filaments and can cross-link actin filaments and microtubules. (A) Low speed pelleting of Crn1p–F-actin complexes. Crn1p (0.5 μM) or Crn1p (Δ600–651; 0.5 μM) was mixed with preassembled yeast actin filaments (2 μM), incubated for 15 min at 25°C, and centrifuged for 3 min at low speed (13,000 *g*). The pellets and supernatants were analyzed by SDS-PAGE and Coomassie staining. (B) Crn1p decreases the apparent viscosity of actin filament solutions in a concentration-dependent manner. Variable concentrations of Crn1p or yeast fimbrin/Sac6p (0.15–2.5 μM) were added to preassembled actin filaments (7 μM), and apparent viscosity was measured by the falling ball assay. (C) Electron micrographs of Crn1p-actin filament bundles and fimbrin/Sac6p-actin filament bundles. Crn1p or Sac6p (0.5 μM) was added to preassembled yeast actin filaments (5 μM), incubated for 30 min at 25°C, then negatively stained and examined by electron microscopy. (D) Cosedimentation of microtubules with Crn1p-F-actin bundles. 4 μM taxol-stabilized microtubules, 4 μM preassembled F-actin, 2 μM Crn1p, and 2 μM Sac6p were mixed in the combinations indicated in the figure and incubated for 30 min at 25°C. The reactions then were centrifuged at low speed (13,000 *g*) for 3 min, and the pellets and supernatants were analyzed by SDS-PAGE gels and Coomassie staining. Bar, 200 nm.

Microtubules Cosediment with Crn1p–F-Actin Bundles

The isolation of Crn1p on microtubule affinity columns suggested that Crn1p can form a stable complex with microtubules, but as documented above (Fig. 2 C), the in vitro binding interaction between microtubules and Crn1p is weak (15–20 μM). To address the possibility that posttranslational modifications of Crn1p might increase the Crn1p binding affinity for microtubules (recombinant Crn1p was used for the studies described above), we performed cosedimentation assays by adding taxol-stabilized bovine brain microtubules to yeast extracts, and after Crn1p cosedimentation by immunoblotting. However, the measured affinity was similar to that in Fig. 2 C (not shown). This prompted us to test whether the third component of the complex isolated on the microtubule affinity column (actin), might stabilize the Crn1p-microtubule binding interaction. First, we tested whether the presence of G-actin (under nonpolymerizing conditions) influenced the affinity of Crn1p for microtubules, but it did not (not shown). Next, we tested the effects of F-actin on the Crn1p-microtubule interaction by assaying for microtubule cosedimentation with Crn1p–F-actin bundles at low speeds. The results are shown in Fig. 3 D, and were quantitated by scanning densitometry.

Background levels of tubulin pelleting (12–18%) were observed in reactions that contained microtubules alone or microtubules in the presence of Sac6p/fimbrin, Crn1p, or F-actin alone (Fig. 3, lanes 1–6). As expected, the addition of Sac6p or Crn1p to actin filaments led to actin filament bundling and pelleting of the actin at low speed (lanes 7–10). Importantly, microtubule pelleting did not increase above background in the presence of Sac6p–F-actin
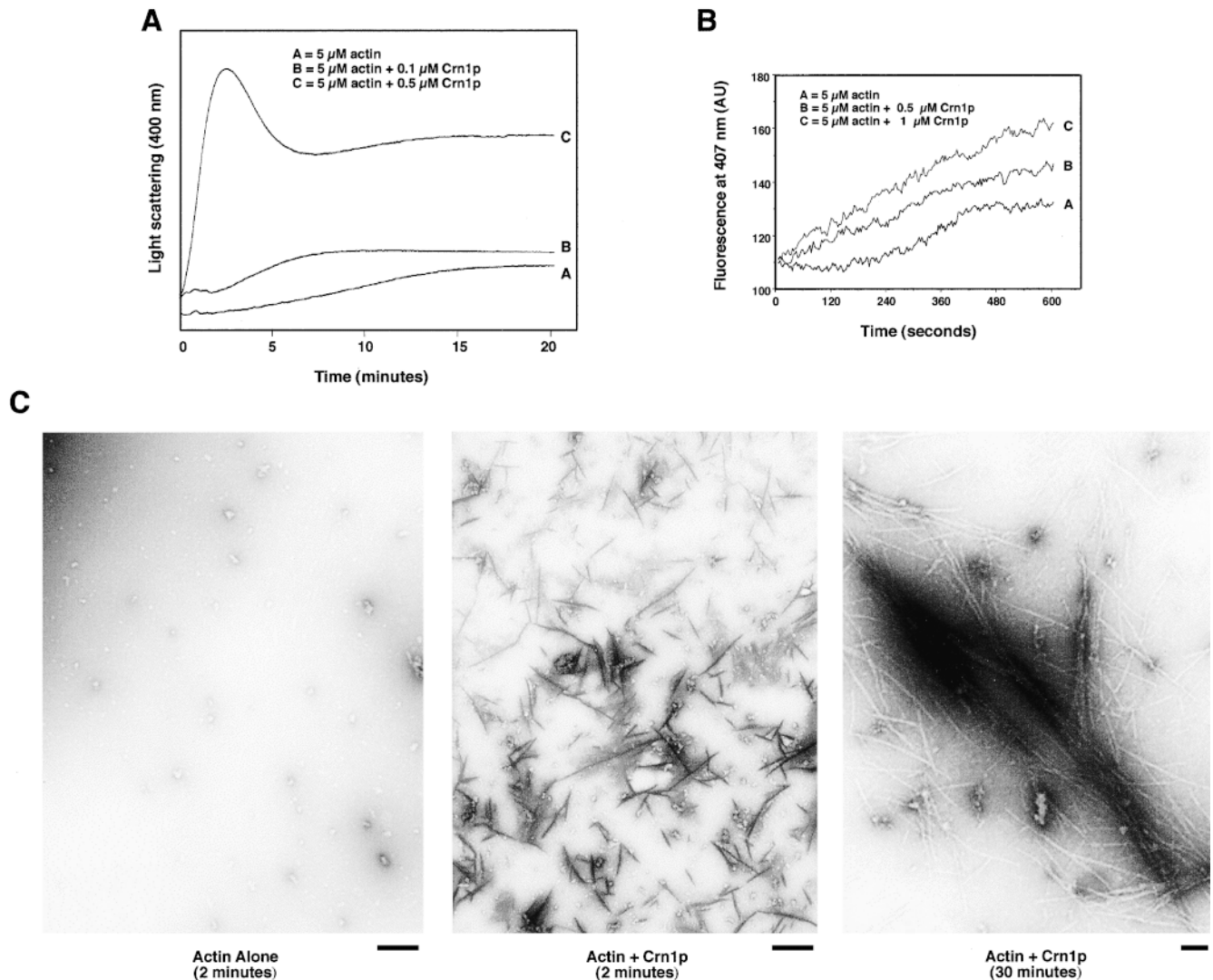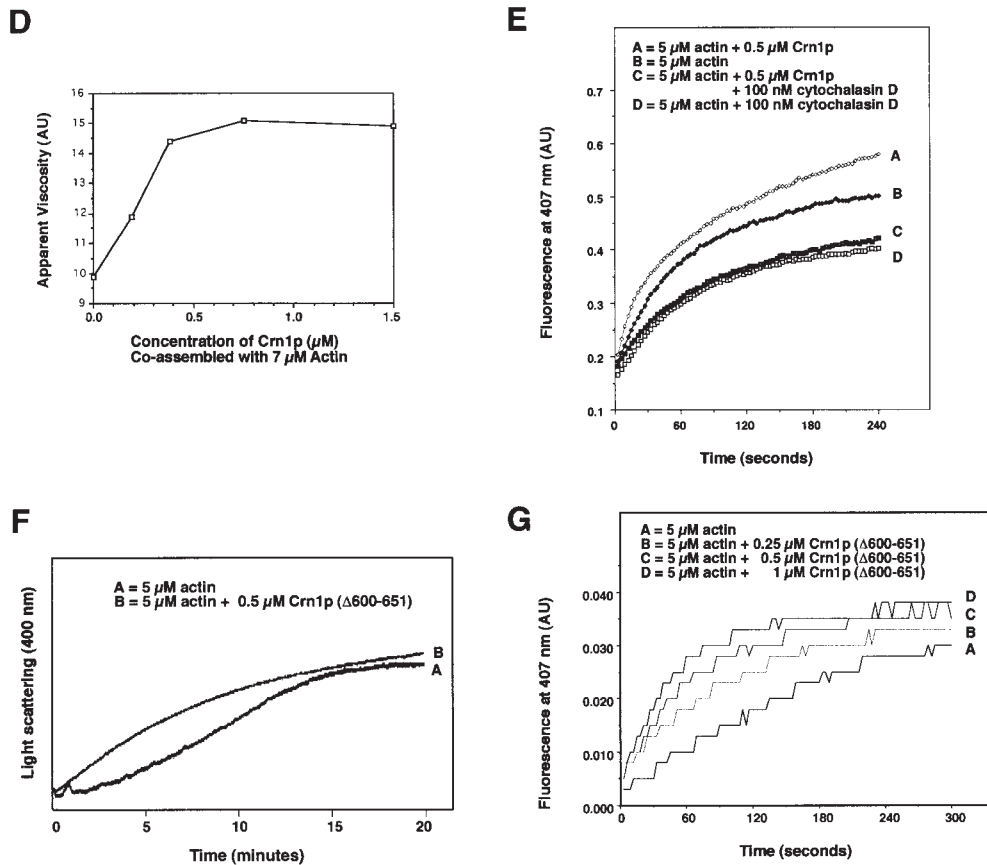
Figure 4. Crn1p promotes the rapid barbed-end assembly and cross-linking of actin filaments into branched networks. (A) Effects of Crn1p on assembly kinetics of yeast actin by light scattering assay. Monomeric yeast actin (5 μm) in G-buffer was mixed with variable concentrations of Crn1p and assembly initiation salts at time 0. Actin filament assembly was monitored by change in light scattering at 400 nm in a spectrophotometer. Steady state actin filament assembly was reached by 20 min in all reactions, and at this point reactions contained similar polymer levels (see Materials and Methods). (B) Effects of Crn1p on the assembly kinetics of pyrene-actin. Variable concentrations of Crn1p (0, 0.5, or 1 μM) were added to 5 μM actin (4 μM yeast actin and 1 μM pyrene-labeled rabbit muscle actin), and actin filament assembly was monitored by increase in pyrene fluorescence (excitation 365 nm/excitation 407 nm). Fluorescence units are arbitrary. (C) Electron micrographs of actin assembly reactions containing 5 μM yeast actin in the absence or presence of 0.5 μM Crn1p. Samples were removed from the assembly reactions at 2 min and at steady state (30 min), fixed in 0.5% glutaraldehyde, negatively stained, and examined by electron microscopy. (D) Crn1p causes a concentration-dependent increase in apparent viscosity when coassembled with actin. Variable concentrations of Crn1p (0.2–1.5 μM) were added to monomeric yeast G-actin (7 μM), incubated for 20 min at 25°C, and apparent viscosity was measured by the falling ball assay. (E) Crn1p induces barbed-end actin filament assembly. The assembly of 5 μM actin (4 μM yeast actin and 1 μM pyrene-labeled rabbit muscle actin) was compared in the presence or absence of 100 nM cytochalasin D, which blocks barbed-end filament assembly, and in the presence or absence of 0.5 μM Crn1p. Assembly was nucleated with preassembled, sheared yeast actin filament seeds (0.5 μM). (F) Effects of Crn1p (Δ600–651) on the kinetics of yeast actin filament assembly measured by light scattering assay. The assembly of monomeric yeast actin (5 μM) was monitored by light scattering as above in the presence or absence of 0.5 μM Crn1p (Δ600–651), which lacks filament cross-linking activity. (G) Effects of Crn1p (Δ600–651) on the kinetics of pyrene-actin assembly. Variable concentrations of Crn1p (Δ600–651; 0, 0.25, 0.5, or 1 μM) were added to 5 μM monomeric actin (4 μM yeast actin and 1 μM pyrene-labeled rabbit muscle actin), and actin filament assembly was monitored by increase in pyrene fluorescence as above. Bar, 200 nm.

bundles (17%; lanes 9 and 10). This reaction serves as a control for nonspecific trapping of microtubules by actin bundles. As shown in lanes 7 and 8, there is a pronounced increase in microtubule pelleting (65%) in the presence of Crn1p–F-actin bundles. This result suggests that Crn1p can directly cross-link microtubules and actin filaments with an apparent affinity of ~2 μM, ~10-fold stronger than the interaction between Crn1p and microtubules in

D

Apparent Viscosity (AU) vs Concentration of Crn1p (μM) Co-assembled with 7 μM Actin

E

A = 5 μM actin + 0.5 μM Crn1p
B = 5 μM actin
C = 5 μM actin + 0.5 μM Crn1p
+ 100 nM cytochalasin D
D = 5 μM actin + 100 nM cytochalasin D

Fluorescence at 407 nm (AU) vs Time (seconds)

F

A = 5 μM actin
B = 5 μM actin + 0.5 μM Crn1p (Δ600-651)

Light scattering (400 nm) vs Time (minutes)

G

A = 5 μM actin
B = 5 μM actin + 0.25 μM Crn1p (Δ600-651)
C = 5 μM actin + 0.5 μM Crn1p (Δ600-651)
D = 5 μM actin + 1 μM Crn1p (Δ600-651)

Fluorescence at 407 nm (AU) vs Time (seconds)

the absence of actin filaments (Fig. 2 C). These results can account for the isolation of a stable Crn1p-actin complex on microtubule affinity columns.

Crn1p Promotes the Rapid Barbed-End Assembly of Actin Filaments and Cross-links Filaments into Complex Networks

Next, we measured the effects of purified Crn1p on the kinetics of yeast actin filament assembly using two different assays, light scattering and pyrene-actin fluorescence. The pyrene-actin assay can be more reliable than light scattering assays because the signal is directly proportional to polymer level, whereas light scattering levels are influenced by filament lengths and bundling. However, the light scattering assay had an advantage because 100% unmodified yeast actin was used, whereas the pyrene-actin assay uses a mixture of yeast actin and pyrene-labeled rabbit muscle actin. In both assays, actin alone exhibited a lag phase of assembly, followed by polymerization that reached steady state by 20 min (Fig. 4, A and B, curve A). The lag phase for actin assembly is attributed to the slow formation of actin dimers and/or trimers required to nucleate filament elongation (Wegner and Engel, 1975; Pollard, 1990).

In both assays, the addition of 0.5 μM Crn1p to 5 μM monomeric actin caused a dramatic increase in the rate of actin filament assembly (Fig. 4, A, curve C and B, curve B). The reduction in the lag-phase caused by Crn1p suggests

that it can nucleate filament assembly and/or accelerate filament elongation. These effects were concentration dependent, since the addition of 0.1 μM Crn1p to 5 μM actin caused a more subtle increase in assembly rate (Fig. 4 A, curve B) than did the addition of 0.5 μM Crn1p (curve C). The increased light scattering at steady state caused by Crn1p (Fig. 4 A, curve C) is expected due to the cross-linking of actin filaments. Minimal cross-linking appeared to occur at Crn1p concentrations of 0.1 μM (Fig. 4 A, curve B), consistent with the minimal effects on apparent viscosity at similar ratios of Crn1p to actin (Fig. 3 B). Pelleting assays showed that >95% of actin in all of the reactions shown in Fig. 4, A and B was polymerized at steady state (see Materials and Methods), indicating that Crn1p did not appreciably increase polymer mass at steady state. Reactions containing Crn1p reached a higher final level of pyrene fluorescence at steady state. Because polymer mass was not affected by Crn1p, it is likely that the increased pyrene signal at steady state is either due to Crn1p-induced bundling of filaments or Crn1p binding to filaments, which might change the local environment of the pyrene. 1 μM Sac6p/fimbrin caused a similar increase in final pyrene-actin fluorescence level without an appreciable increase in polymer mass (not shown).

We also examined by electron microscopy samples from actin assembly reactions at an early (2 min) time point (Fig. 4 C). No filaments were visible in reactions containing 5 μM yeast actin alone at 2 min, consistent with the lag phase for assembly. In contrast, numerous short filaments
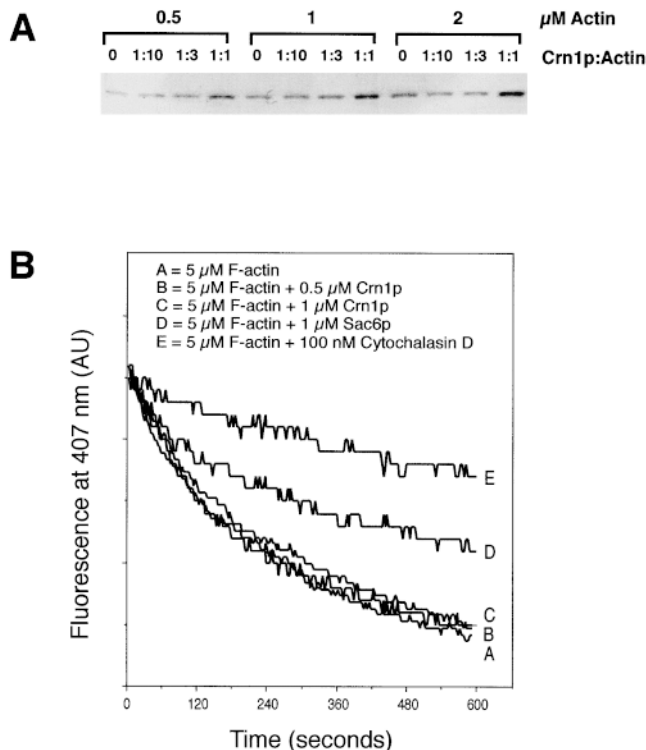
A

	0.5			1			2			*μM* Actin
0	1:10	1:3	1:1	0	1:10	1:3	1:1	0	1:10	1:3	1:1	Crn1p:Actin

B

A = 5 μM F-actin
B = 5 μM F-actin + 0.5 μM Crn1p
C = 5 μM F-actin + 1 μM Crn1p
D = 5 μM F-actin + 1 μM Sac6p
E = 5 μM F-actin + 100 nM Cytochalasin D

Figure 5. Crn1p has no significant effects on actin critical concentration (actin Cc) at steady state or the rate of actin filament depolymerization. (A) Crn1p does not affect significantly the actin Cc at steady state. Three different concentrations of preassembled yeast actin filaments (0.5, 1, or 2 μM) were mixed with four different molar ratios of Crn1p to actin (0, 1:10, 1:3, 1:1), incubated for 20 min, and the actin filaments in the reactions were pelleted by high speed centrifugation. Levels of unpolymerized actin (actin in the supernatant) were compared by SDS-PAGE and Coomassie staining. (B) Crn1p does not affect the rate of actin filament depolymerization. 5 μM preassembled F-actin (4 μM yeast actin and 1 μM pyrene-labeled rabbit muscle actin) was added to 0.5 μM Crn1p, 1 μM Crn1p, 1 μM Sac6p/fimbrin, or 100 nM cytochalasin D. After incubation for 15 min at 25°C, filament disassembly was induced by the addition of 40 μM latrunculin A at time 0, and depolymerization was monitored by change in pyrene fluorescence as described in Fig. 4 b.

that appeared bundled were visible in the reactions containing 0.5 μM Crn1p and 5 μM yeast actin. This result strongly supports the conclusion that Crn1p promotes rapid actin filament assembly. Interestingly, branching of the short filaments was evident by the 2-min time-point of assembly; this could be an important aspect of how coronin influences the formation of actin structures in vivo. Examination of the same reactions at steady state (30 min) revealed branched networks of bundled and cross-linked short filaments. The appearance of these actin networks contrasted markedly with the appearance of preassembled actin filaments to which Crn1p is added (Fig. 3 D). This observed difference prompted us to measure the effects of Crn1p on apparent viscosity in coassembly reactions. As shown in Fig. 4 D, Crn1p caused a concentration-dependent increase in viscosity, consistent with the formation of the branched filament networks visualized by electron mi-

croscopy. The effect is opposite to that observed when Crn1p was added to preassembled actin filaments, which led to a concentration-dependent decrease in viscosity (Fig. 3 B). Thus, Crn1p has the capacity to form either smooth bundles of long actin filaments or networks of branched and bundled short filaments, with decreased or increased apparent viscosity, respectively.

To determine from which end of the filament Crn1p-induced actin assembly occurs, we measured pyrene-actin assembly in the presence and absence of 100 nM cytochalasin D. At this concentration, cytochalasin D blocks barbed-end assembly, limiting polymerization to pointed ends (Cooper, 1987). We monitored the assembly of 5 μM actin (4 μM yeast actin and 1 μM pyrene-labeled rabbit muscle actin) in the presence or absence of 100 nM Cytochalasin D and the presence or absence of 0.5 μM Crn1p. Assembly was nucleated by the addition of 0.5 μM preassembled, sheared yeast actin filament seeds. As shown in Fig. 4 E, the addition of cytochalasin D to the reactions led to a similar decrease in the rate of actin polymerization with and without Crn1p. This shows that Crn1p induces barbed end assembly of actin filaments.

Next, we tested the effects on actin assembly of a truncated Crn1p (Crn1p Δ600–651) that binds to actin filaments but lacks cross-linking activity (see Figs. 3 A and 6). Crn1p Δ600–651 increased the rate of actin assembly in both light scattering (Fig. 4 F) and pyrene-actin assembly assays (Fig. 4 G), significantly reducing the lag phase of actin assembly. This demonstrates that assembly-promoting activity is independent of cross-linking activity.

Crn1p Does Not Stabilize Actin Filaments or Change the Steady State Actin Critical Concentration

To test whether Crn1p has any effects on filament stability, we first measured the effect of Crn1p on the critical concentration for actin assembly (actin Cc). Actin Cc is defined as the concentration of actin above which it assembles into polymer. In sedimentation assays, this corresponds to the concentration of actin in the supernatant after high speed centrifugation. As shown in Fig. 5 A, Crn1p caused no significant change in actin Cc at molar ratios of 1:10 and 1:3 Crn1p to actin. There was a small increase in the actin Cc (less than twofold) at 1:1 molar ratios. However, this effect may not be relevant in vivo since Crn1p is present in yeast at a molar ratio of 1 Crn1p per 10 actin subunits.

To measure the effects of Crn1p on filament stability, we assayed the disassembly of preassembled pyrene-actin filaments mixed with 0.5 or 1 μM Crn1p, 1 μM Sac6p (a known F-actin stabilizing protein) or 100 nM cytochalasin D, which blocks barbed ends. The filaments were then mixed with 40 μM latrunculin A (an actin monomer-sequestering agent) and filament disassembly was monitored by pyrene fluorescence. As shown in Fig. 5 B, fimbrin/Sac6p (curve D) and cytochalasin D (curve E) stabilized filaments, reducing their rates of depolymerization, but Crn1p did not affect the rate of filament depolymerization (curves B and C).

Crn1p Activities are Mediated by Distinct Domains

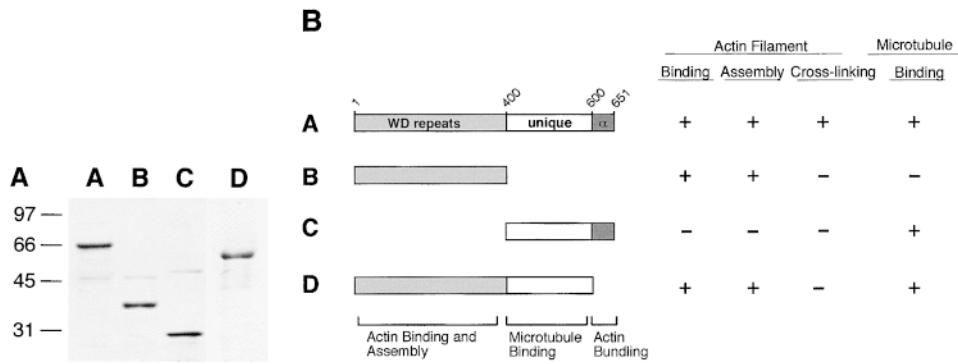To further dissect Crn1p function, we expressed fragments

Figure 6. Activities of Crn1p domains. (A) Coomassie-stained SDS-PAGE gel of Crn1p and Crn1p subfragments expressed and purified from *E. coli.* A = full-length (amino acids 1–651), B = 1–400, C = 400–651, and D = 1–599. (B) Biochemical activities of Crn1p polypeptides. Each polypeptide was tested for microtubule and F-actin binding by cosedimentation assay, ability to promote F-actin assembly by light scattering assay, and actin filament bundling by low speed pelleting assay and electron microscopy.

of Crn1p (amino acids 1–600, 1–400, and 400–651) in *E. coli* and purified each fragment as described above for full-length Crn1p (Fig. 6 A). Each fragment was tested in vitro for its ability to (a) cosediment with microtubules, (b) cosediment with actin filaments, (c) promote actin filament assembly by light scattering assay and (d) bundle actin filaments by low speed pelleting assays and electron microscopy. The results are summarized in Fig. 6 B. Two fragments missing COOH-terminal sequences, Crn1p (Δ400–651) and Crn1p (Δ600–651), the later consisting of only the WD-repeat region, demonstrated F-actin binding and assembly-promoting activities. The COOH terminus (400–651), which contains the MAP1B-homologous re-

gion, is both required and sufficient for microtubule binding. The COOH-terminal coiled-coil region (600–651) is required for actin bundling. This result suggests that actin filament cross-linking may depend on coiled coil mediated Crn1p dimerization.

Crn1p Localizes to the Yeast Cortical Actin Cytoskeleton In Vivo

Crn1p localization in wild-type yeast cells was examined by immunofluorescence microscopy using anti-Crn1p antibodies (Fig. 7). Crn1p localized to punctate structures at the cell cortex throughout the cell cycle, and staining was absent in *crn1Δ* cells. Double label immunofluorescence microscopy with anti-actin antibodies showed that these punctate structures correspond to cortical actin patches. Furthermore, direct fluorescence microscopy of cells expressing a GFP-Crn1p fusion protein showed a similar localization pattern (not shown) and the GFP-Crn1p staining patches were motile. The motility of cortical actin patches in *S. cerevisiae* has been established previously (Doyle and Botstein, 1996; Waddle et al., 1996), and the variable motility rates of the GFP-Crn1p staining patches were similar to those observed for actin patches. Addition of latrunculin A to cells caused the rapid disassembly of the actin cytoskeleton and concomitant translocation of Crn1p staining to the cytoplasm (not shown). Double label immunofluorescence microscopy showed that Crn1p localization to cortical actin patches is unaffected by a number of mutations in genes encoding actin cytoskeleton proteins, including *abp1Δ*, *aip1Δ*, *cap2Δ*, *cof1-22*, *pfy1-116*, *sac6Δ*, *srv2Δ*, *rvs161Δ*, *rvs167Δ*, *sla1Δ*, *sla2Δ*, and *tpm1Δ* (not shown).

Synthetic Defects in Actin Organization Between a CRN1 Gene Disruption Mutation and Mutations that Reduce Actin Filament Turnover Rates

Deletion of the *CRN1* gene resulted in no obvious defects in cell morphology or growth rate at 16, 20, 25, 30, 34, and 37°C. Moreover, *crn1Δ* cells grew indistinguishably from wild-type cells on medium supplemented with 1 M NaCl, 1 M KCl, 0.1 M MgCl$_2$, 0.1 M CaCl$_2$, 1 M sorbitol, or 3% formamide, and exhibited normal fluid phase endocytosis,
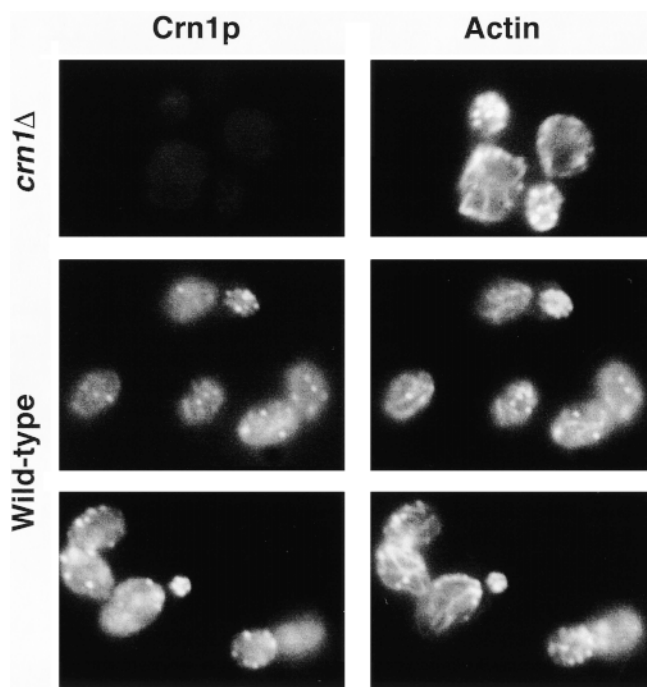

Figure 7. Localization of Crn1p in yeast cells. Actin and Crn1p localization in wild-type (DDY1088) and *crn1Δ* (DDY1521) strains was examined by double-label immunofluorescence microscopy using Crn1p and actin antibodies.
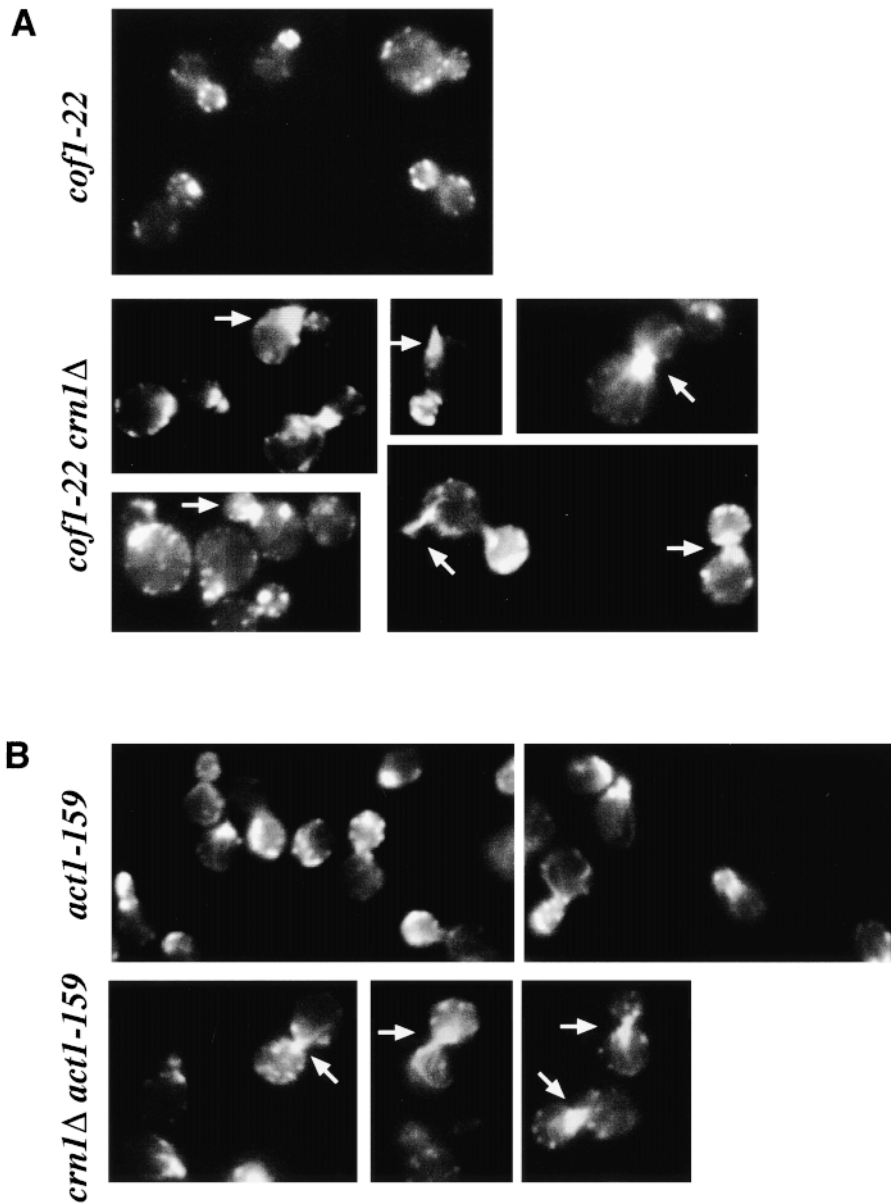
A

cof1-22

cof1-22 crn1Δ

B

act1-159

crn1Δ act1-159

Figure 8. Synthetic defects in actin organization in *crn1Δ cof1-22* and *crn1Δ act1-159* cells. Haploid segregants from *crn1Δ × cof1-22* and *crn1Δ × act1-159* genetic crosses were grown to log phase at 20°C, and actin organization was examined by rhodamine phalloidin staining. *crn1Δ* cells and wild-type cells had normal actin staining (not shown). Actin staining is shown for *cof1-22* and *cof1-22 crn1Δ* cells (A) and for *act1-159* and *act1-159 crn1Δ* cells (B). Arrows mark defects in actin organization specific to the double mutants.

as monitored by uptake of lucifer yellow dye. The actin cytoskeletons of *crn1Δ* cells also appeared normal when examined by actin immunofluorescence (Fig. 7). Given the high affinity of Crn1p for actin filaments in vitro and its dramatic effects on actin assembly, the absence of a detectable defect in actin organization or cell growth in *crn1Δ* cells suggested there may be proteins in yeast whose functions are redundant with Crn1p function.

To test this possibility, we crossed *crn1Δ* strains to strains with mutations in genes encoding other actin-associated proteins (*abp1Δ*, *aip1Δ*, *cap2Δ*, *cof1-22*, *las17Δ*, *pca1Δ*, *pfy1-116*, *sac6Δ*, *rvs167Δ*, *tpm1Δ*, and *twf1Δ*). Haploid progeny from crosses were compared for growth at 16, 20, 25, 30, 34, and 37°C, and examined by rhodamine phalloidin staining for defects in actin cytoskeleton organization. Only one mutant, *cof1-22*, showed synthetic defects in combination with *crn1Δ*. *cof1-22* is an allele of the cofilin gene that results in a partial defect in actin filament depolymerization/severing, resulting in slower turnover of

actin filaments (Lappalainen and Drubin, 1997). At 25°C, *cof1-22* cells have normal morphologies, show a partial depolarization of their cortical actin patches (~25% of cells), and their actin patches appear somewhat brighter than patches in wild-type cells (Fig. 8 A). *cof1-22 crn1Δ* double mutant cells grew more slowly than *cof1-22* cells and were generally larger and more rounded. In addition, many of the double mutant cells accumulated a large mass of filamentous actin near the bud neck (Fig. 8 A, arrows). Some cells also had multiple buds, elongated necks, and/or abnormal protrusions of actin staining (Fig. 8 A, arrows).

The *crn1Δ cof1-22* genetic interaction prompted us to test for interactions between *crn1Δ* and *act1-159*, a mutation that resides in the ATP binding pocket of actin. The *act1-159* mutation shows genetic interactions with *cof1-22* and reduces the turnover of actin filaments (Belmont and Drubin, 1998). At 25°C, *act1-159* cells grow more slowly than wild-type cells, they show partially delocalized cortical actin patch staining, and have somewhat brighter actin

patch and cable staining than wild-type cells (Fig. 8 B). *act1-159 crn1Δ* double mutant cells grow more slowly than *act1-159* cells and show severe defects in actin organization. The majority of *act1-159 crn1Δ* cells show a reduction in actin staining intensity of their cortical actin patches, and many cells accumulate a large filamentous actin mass near their bud necks (Fig. 8 B, arrows).

Defects in *crn1Δ* Cells Suggest a Microtubule Function for Crn1p

Examination of microtubule staining in *crn1Δ* cells by immunofluorescence revealed defects in cytoplasmic microtubule orientation and length (Fig. 9). Approximately 5% of the medium- to large-budded *crn1Δ* cells showed unusually long and misoriented cytoplasmic microtubules that extended from the SPB in the bud back towards or through the neck into the mother cell. This result is quite dramatic since similar defects were never seen in wild-type cells ($n > 1,000$ cells).

Overexpression of GST-Crn1p Causes an Arrest of Cell Growth and Severe Defects in Actin and Microtubule Organization

To test the effects of overexpression of Crn1p, a GST-Crn1p fusion protein was expressed in wild-type yeast
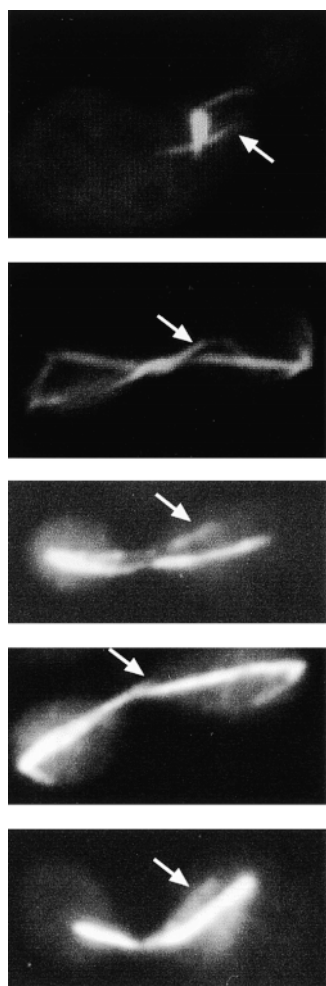

Figure 9. Deletion of the *CRN1* gene causes pronounced defects in cytoplasmic microtubules at a low frequency. Wild-type (DDY-1519) and *crn1Δ* (DDY1518) cells were grown at 20°C to $OD_{600} = 0.5$ and examined by immunofluorescence microscopy using tubulin antibodies. Approximately 5% of the medium to large budded *crn1Δ* cells had abnormally long cytoplasmic microtubules (marked by arrows) that emanate from the microtubule organizing center in the bud and extend back towards or through the bud neck into the mother cell. Similar defects were never seen in the wild-type cells ($n > 1,000$ cells).

(DDY130) on a high copy plasmid under the regulation of the *GAL10* promoter. Cells expressing GST alone showed normal morphologies and normal microtubule and actin organization. However, overproduction of GST-Crn1p led to an arrest of cell growth and to dramatic changes in cell morphology. Approximately 50% of the cells became extremely large and rounded, and almost every cell, normal in size or enlarged, showed severe defects in actin and microtubule organization as shown by double label immunofluorescence microscopy (Fig. 10). In these cells, the cortical actin patches were depolarized, actin cables were not visible, and the majority of cells contained a single abnormal actin bar-like structure located in or near the nucleus. Intriguingly, these abnormal structures often appeared to be coincident with or proximal to tubulin bar-like structures. These cell populations also showed a striking absence of medium or long spindles, raising the possibility that the activities of Crn1p at the cortical actin cytoskeleton help to regulate spindle elongation.

Discussion

Coronin Promotes the Rapid Assembly and Cross-linking of Actin Filaments

Coronin is a highly conserved actin-associated protein that localizes to sites of dynamic actin assembly in *D. discoideum* and to the actin tails of *Listeria* in infected mammalian cells (see Introduction). However, until now, no activities other than actin binding had been demonstrated for coronin. Here, we have identified an *S. cerevisiae* homologue of coronin, Crn1p, and have shown that it (a) localizes to the yeast cortical actin cytoskeleton, (b) binds to actin filaments with high affinity ($K_d \sim 6$ nM), and (c) promotes the rapid barbed end assembly and cross-linking of actin filaments. These two activities (assembly-stimulation and cross-linking) are mediated by distinct domains in Crn1p. Because both domains are highly conserved, these activities are likely to be conserved in all members of the coronin family.

We have shown that actin filament cross-linking depends on the coiled-coil domain of Crn1p, suggesting a requirement for Crn1p dimerization. This model is supported further by the coimmunoprecipitation of native coronin from yeast extracts with an epitope-tagged Crn1p expressed in these cells (B.L. Goode, D.G. Drubin, and G. Barnes, unpublished results). Crn1p is capable of cross-linking actin filaments in vitro into branched networks or smooth bundles of filaments, depending on whether Crn1p is present during the assembly of actin, or is added after actin assembly, respectively. One implication of this analysis is that coronin could organize actin filaments into different higher order structures depending on cellular conditions or signals.

Coronin Promotes the Rapid Barbed-End Assembly of Actin Filaments by a Novel Mechanism

Crn1p significantly reduces the lag phase for actin filament assembly. This activity is independent of coronin's filament cross-linking activity, since Crn1p (Δ600–651) has full assembly activity, but does not cross-link filaments.

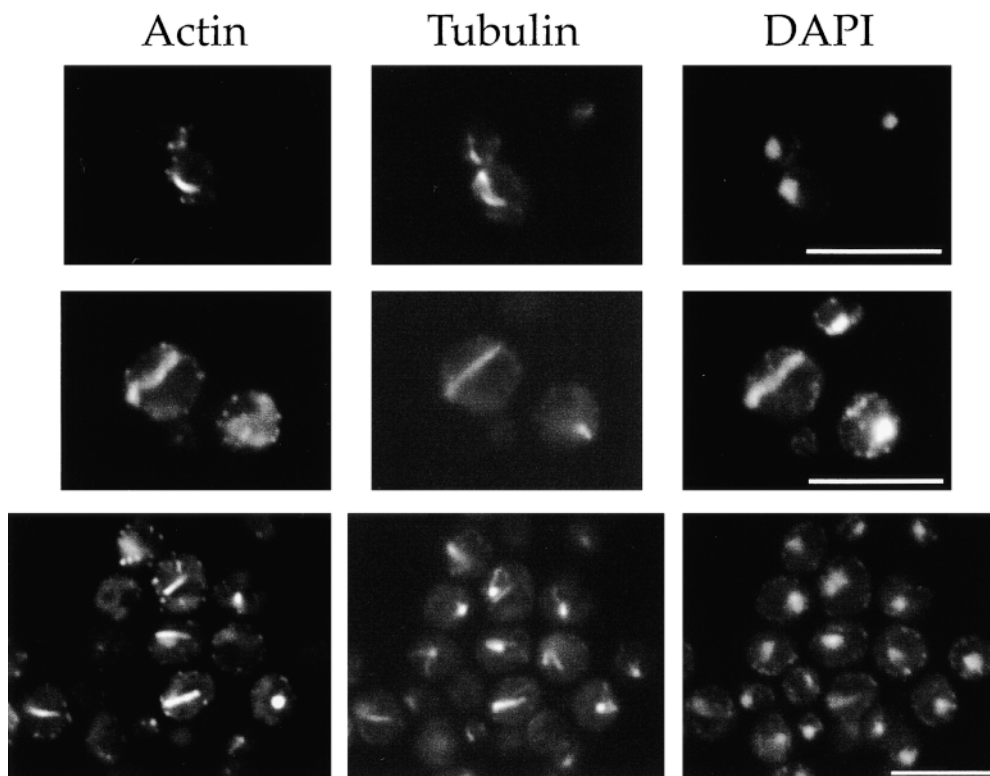| Actin	Tubulin	DAPI

Figure 10. Overexpression of GST-Crn1p causes severe defects in cell growth and microtubule and actin organization. Wild-type cells (DDY-130) carrying the pEGKT-CRN1 plasmid were grown to log phase at 25°C in minimal selective medium (lacking uracil and leucine) with glucose. Cells were washed and transferred to minimal selective medium with 2% raffinose for 12 h of growth at 25°C. Then 2% galactose was added to induce the expression of GST-Crn1p. After 4 h growth at 25°C, the cells were examined by double label immunofluorescence microscopy using actin and tubulin antibodies. Bar, 10 μM.

Further, we have shown that a different actin filament bundling protein (yeast fimbrin/Sac6p) has no effect on actin assembly (Goode, B.L., D.G. Drubin, and G. Barnes, unpublished data). Thus, the effects of coronin on actin assembly are specific and unrelated to cross-linking.

The assembly lag phase has been attributed to the slow and reversible formation of actin dimers and/or trimers (Wegner and Engel, 1975; Pollard and Cooper, 1986). Crn1p might reduce the lag phase for assembly by increasing the rate of formation of dimers/trimers and/or free ends of filaments available for polymerization. An increase in available filament ends can be accomplished in vitro by severing of filaments, capping of filament ends to stabilize dimer/trimer formation, or binding to the sides of dimers/trimers to stabilize their formation. Our data argue strongly against a filament severing or capping mechanism for Crn1p. Severing proteins, including the gelsolin/villin/severin family and the ADF/cofilin family (reviewed in Hartwig and Kwiatkowski, 1991; Carlier, 1998), increase the rate of filament depolymerization, and when added to preassembled actin filaments, sever and/or depolymerize filaments to reduce the average length of filaments. In contrast, coronin has no detectable effects on the rate of filament depolymerization, and shows no indication of severing and/or inducing depolymerization when it is added to preassembled filaments.

Coronin also does not have properties of a capping protein. Barbed end capping proteins increase the actin critical concentration and reduce the rate of filament depolymerization, and do so at low stoichiometries of capping protein to actin (Schafer et al., 1996). Pointed end capping proteins, such as the Arp2/3 complex, also dramatically re-

duce the rate of depolymerization of filaments at low stoichiometries (Mullins et al., 1998). In contrast, coronin has no significant effect on the actin critical concentration or the rate of depolymerization of filaments. Barbed-end capping proteins also reduce the rate of filament elongation, since they limit polymerization to the pointed ends. However, Crn1p-induced filament assembly is rapid and occurs by addition of actin subunits at the barbed ends of filaments. These data argue strongly against coronin having capping and/or severing activities. Thus, if coronin does increase the number of free ends available for polymerization, it likely does so by stabilization of actin dimers/trimers via interactions with their sides.

An alternate, but not mutually exclusive mechanism to explain the reduction in assembly lag phase by coronin is that it increases the rate of actin filament elongation. The rates of actin polymerization observed in neutrophil cell extracts suggest that there may be cellular factors that accelerate actin filament elongation (Zigmond, 1998; Zigmond et al., 1998). However, until now, no protein possessing the appropriate biochemical activities to mediate this effect has been isolated. Although the Arp2/3 complex mixed with the ActA protein from *Listeria monocytogenes* promotes extremely rapid actin filament assembly in vitro (Welch et al., 1998), it is not yet clear whether these effects are due to nucleation and/or increased rates of elongation. We speculate that Crn1p acts by binding to the sides of and stabilizing actin dimers/trimers, and/or accelerating filament elongation. That coronin binds to the sides of actin filaments is supported by the 1:1 saturation stoichiometry of coronin binding to actin and by mapping of the coronin binding site on actin (Goode, B.L., and D.G. Drubin,

unpublished data). It is less clear how coronin might increase the rate of filament elongation.

Genetic Analyses Are Consistent with a Role for Crn1p in Regulating the Assembly and Turnover of the Cortical Actin Cytoskeleton

Although Crn1p has potent activities on actin in vitro, deletion of the *CRN1* gene causes no detectable defects in actin organization, endocytosis, or cell growth. The lack of a readily detectable null phenotype in cells could be explained if Crn1p function is redundant with other proteins in yeast. This is not uncommon for yeast actin-associated proteins (e.g., Abp1p, Aip1p, Myo3p, Myo4p, Myo5p, and Twf1p). However, the *crn1Δ* mutation showed no obvious synthetic defects in combination with mutations in *ABP1*, *AIP1*, *CAP2*, *LAS17*, *PFY1*, *PCA1*, *SAC6*, *RVS167*, or *TWF1*, suggesting that *CRN1* may have functions distinct from those mediated by these genes.

Specific genetic interactions were observed between a *crn1Δ* mutation and the *cof1-22* (Lappalainen and Drubin, 1997) and *act1-159* (Belmont and Drubin, 1998) mutations. Given that cofilin promotes the rapid disassembly of actin filaments at their pointed ends (Carlier, 1998) and that coronin promotes the rapid assembly of actin filaments at their barbed ends, we speculate that the genetic interaction between coronin and cofilin may result from a loss of complementary activities directed at opposite ends of the filament. The combination of reduced assembly-promoting activity and reduced filament disassembly (and therefore, a reduced actin monomer pool) may impair the capacity to form new filaments. Similarly, this might explain the genetic interaction between the *crn1Δ* and *act1-159* mutations, since *act1-159* also reduces the rate of actin filament disassembly and turnover in vivo (Belmont and Drubin, 1998).

The activities that we have demonstrated for coronin also raise the possibility of a functional interaction between coronin and the Arp2/3 complex and/or WASP, two key regulators of actin assembly (Symons et al., 1996; Welch et al., 1997, 1998; Mullins et al., 1998; reviewed in Zigmond, 1998). The defects in actin organization in *cof1-22 crn1Δ* and *act1-159 crn1Δ* cells (accumulation of a large mass of actin near the bud neck) are similar to those in mutants of the Arp2/3 complex (*arp3-2*; Winter et al., 1997) and mutants of the yeast WASP homologue, *LAS17/BEE1* (Li, 1997; M. Duncan and D.G. Drubin, unpublished results). Further, coronin copurifies with the Arp2/3 complex from neutrophil extracts (Machesky et al., 1997), suggesting a possible direct interaction.

Crn1p May Help Link the Actin and Microtubule Cytoskeletons in Yeast

Several observations lead us to consider that yeast coronin may have an additional role in linking functions of the actin and microtubule cytoskeletons in yeast. First, the unique region of Crn1p shares sequence homology with the microtubule binding region of MAP1B and is required for microtubule binding by Crn1p. Second, in the presence of actin filaments, the microtubule binding affinity of Crn1p is enhanced markedly. Despite the low penetrance of the microtubule phenotype, the defects are distinct and specific; similar defects are never observed in wild-type cells. In addition, a different microtubule defect (increase in the number of large-budded cells with short spindles) recently was reported for coronin null mutants (H.-Chapdelaine et al., 1998). To our knowledge, coronin is the first yeast actin binding protein that, when mutated, gives rise to microtubule defects. Coronin also is the first yeast actin binding protein that results in microtubule defects when overexpressed (loss of medium and long spindles and formation of aberrant tubulin-staining structures). Taken together, these biochemical and genetic observations suggest a microtubule function for Crn1p, possibly in attaching cytoplasmic microtubules to cortical actin patches during spindle elongation and nuclear migration. The mild phenotype in the coronin null mutant cells suggests that other factors must be involved in coronin functions, which we will attempt to identify in the future.

References

Ayscough, K.R., and D.G. Drubin. 1997. Immunofluorescence microscopy of yeast cells. *In* Cell Biology, A Laboratory Handbook. Academic Press. San Diego, CA.

Ayscough, K.R. 1998. In vivo functions of actin-binding proteins. *Curr. Opin. Cell Biol.* 10:102–111.

Ayscough, K.R., J. Stryker, N. Pokala, M. Sanders, P. Crews, and D.G. Drubin. 1997. High rates of actin filament turnover in budding yeast and roles for actin in establishment and maintenance of cell polarity revealed using the actin inhibitor latrunculin A. *J. Cell Biol.* 137:399–416.

Barnes, G., K. Andrea Louie, and D. Botstein. 1992. Yeast proteins associated with microtubules in vitro and in vivo. *Mol. Biol. Cell.* 3:29–47.

Belmont, L., and D.G. Drubin. 1998. The yeast V159N actin mutant reveals roles for actin dynamics in vivo. *J. Cell Biol.* 142:1289–1299.

Botstein, D., D. Amberg, J. Mulholland, T. Huffaker, A. Adams, D. Drubin, and T. Stearns. 1997. The yeast cytoskeleton. *In* The Molecular and Cellular Biology of the Yeast *Saccharomyces*. Cold Spring Harbor Lab Press, Cold Spring Harbor, NY. 1–90.

Carlier, M.-F. 1998. Control of actin dynamics. *Curr. Opin. Cell Biol.* 10:45–51.

Carminati, J.L., and T. Stearns. 1997. Microtubules orient the mitotic spindle in yeast through dynein-dependent interactions with the cell cortex. *J. Cell Biol.* 138:629–641.

Cooper, J.A. 1987. Effects of cytochalasin and phalloidin on actin. *J. Cell Biol.* 105:1473–1478.

David, V., E. Gouin, M. VanTroys, A. Grogan, A.W. Segal, C. Ampe, and P. Cossart. 1998. Identification of cofilin, coronin, Rac and capZ in actin tails using a *Listeria* affinity approach. *J. Cell Sci.* 111:2877–2884.

de Hostos, E.L., B. Bradtke, F. Lattspeich, R. Guggenheim, and G. Gerisch. 1991. Coronin, an actin binding protein of *Dictyostelium discoideum* localized to cell surface projections, has sequence similarities to G protein β subunits. *EMBO (Eur. Mol. Biol. Organ.) J.* 10:4097–4104.

de Hostos, E.L., C. Rehfueb, B. Bradtke, D.R. Waddell, R. Albrecht, J. Murphy, and G. Gerisch. 1993. *Dictyostelium* mutants lacking the cytoskeletal protein coronin are defective in cytokinesis and cell motility. *J. Cell Biol.* 120:163–173.

Doyle, T., and D. Botstein. 1996. Movement of yeast cortical actin cytoskeleton visualized *in vivo*. *Proc. Natl. Acad. Sci. USA.* 93:3886–3891.

Dulic, V., M. Egerton, I. Elguindi, S. Raths, B. Singer, and H. Riezman. 1991. Yeast endocytosis assays. *Methods Enzymol.* 194:697–710.

Gavin, R.H. 1997. Microtubule-microfilament synergy in the cytoskeleton. *Int.*

Rev. Cytol. 173:207–242.

Gerisch, G., R. Albrecht, C. Heizer, S. Hodgkinson, and M. Maniak. 1995. Chemoattractant-controlled accumulation of coronin at the leading edge of *Dictyostelium* cells monitored using a green fluorescent protein-coronin fusion protein. *Curr. Biol.* 5:1280–1285.

Guthrie, C., and R. Fink. 1991. Guide to yeast genetics and molecular biology. *Methods Enzymol.* 194:1–933.

H.-Chapdelaine, R.A., N.K. Tran, and J.A. Cooper. 1998. The role of *Saccharomyces cerevisiae* coronin in the actin and microtubule cytoskeletons. *Curr. Biol.* 8:1281–1284.

Hacker, U., R. Albrecht, and M. Maniak. 1997. Fluid-phase uptake by macropinocytosis in *Dictyostelium*. *J. Cell Sci.* 110:105–112.

Hartwig, J.H., and D.J. Kwiatkowski. 1991. Actin-binding proteins. *Curr. Opin. Cell Biol.* 3:87–97.

Karpova, T.S., K. Tatchell, and J.A. Cooper. 1995. Actin filaments in yeast are unstable in the absence of capping protein or fimbrin. *J. Cell Biol.* 131:1483–1493.

Lappalainen, P., and D.G. Drubin. 1997. Cofilin promotes rapid actin filament turnover *in vivo*. *Nature.* 388:78–82.

Li, R. 1997. Bee1, a yeast protein with homology to Wiscott-Aldrich syndrome protein, is critical for the assembly of cortical actin cytoskeleton. *J. Cell Biol.* 136:649–658.

Machesky, L.M., E. Reeves, F. Wientjes, F.J. Mattheyse, A. Grogan, N.F. Totty, L. Burlingame, J.J. Hsuan, and A.W. Segal. 1997. Mammalian actin-related protein 2/3 complex localizes to regions of lamellipodial protrusion and is composed of evolutionarily conserved proteins. *Biochem. J.* 328:105–112.

Maniak, M., R. Rauchenberger, R. Albrecht, J. Murphy, and G. Gerisch. 1995. Coronin involved in phagocytosis: dynamics of particle-induced relocalization visualized by a green fluorescent protein tag. *Cell.* 83:915–924.

McCormack, A.L., D.M. Schieltz, B.L. Goode, S. Yang, G. Barnes, D.G. Drubin, and J.R. Yates. 1997. Direct analysis and identification of proteins in mixtures by LC/MS/MS and database searching at the low-femtomole level. *Anal. Chem.* 69:767–776.

Miller, K.G., C.M. Field, B.M. Alberts, and D.R. Kellogg. 1991. Use of actin filament and microtubule affinity chromatography to identify proteins that bind to the cytoskeleton. *Methods Enzymol.* 196:303–319.

Mitchell, D.A., T.K. Marshall, and R.J. DeSchenes. 1993. Vectors for the inducible over-expression of glutathione S-transferase fusion proteins in yeast. *Yeast.* 9:715–723.

Mitchison, T., and M.W. Kirschner. 1984. Microtubule assembly nucleated by isolated centrosomes. *Nature.* 312:232–237.

Mullins, R.D., J.A. Heuser, and T.D. Pollard. 1998. The interaction of Arp2/3 complex with actin: nucleation, high affinity pointed end capping, and formation of branching networks of filaments. *Proc. Natl. Acad. Sci. USA.* 95:6181–6186.

Neer, E.J., C.J. Schmidt, R. Nambudripad, and T.F. Smith. 1994. The ancient regulatory-protein family of WD-repeat proteins. *Nature.* 371:297–300.

Noble, M., S.A. Lewis, and N.J. Cowan. The microtubule binding domain of microtubule-associated protein MAP1B contains a repeated sequence motif unrelated to that of MAP2 and tau. *J. Cell Biol.* 109:3367–3376.

Okumura, M., C. Kung, S. Wong, M. Rodgers, and M.L. Thomas. 1998. Definition of family of coronin-related proteins conserved between humans and mice: close genetic linkage between coronin-2 and CDC45-associated protein. *DNA Cell Biol.* 17:779–787.

Palmer, R.E., M. Koval, and D. Koshland. 1989. The dynamics of chromosome movement in the budding yeast *Saccharomyces cerevisiae*. *J. Cell Biol.* 109:3355–3366.

Pearson, W.R., and D.J. Lipman. 1988. Improved tools for biological sequence comparison. *Proc. Natl. Acad. Sci. USA.* 85:2444–2448.

Peränen, J., M. Rikkonen, M. Hyvönen, and L. Kääriäinenen. 1996. T7 vectors with a modified T7lac promoter for expression of proteins in *Escherichia coli*. *Anal. Biochem.* 236:371–373.

Pollard, T.D., and J.A. Cooper. 1982. Methods to characterize actin filament networks. *Methods Enzymol.* 85:211–233.

Pollard, T.D., and J.A. Cooper. 1986. Actin and actin-binding proteins: A critical evaluation of mechanisms and functions. *Annu. Rev. Biochem.* 55:987–1035.

Pollard, T.D. 1990. Actin. *Curr. Opin. Cell Biol.* 2:33–40.

Pollard, T.D. 1993. Actin and actin binding proteins. *In* Guidebook to the Cytoskeletal and Motor Proteins. T. Kreis and R. Vale, editors. Oxford University Press. 3–11.

Read, E.B., H.H. Okamura, and D.G. Drubin. 1992. Actin- and tubulin-dependent functions during *Saccharomyces cerevisiae* mating projection formation. *Mol. Biol. Cell.* 3:429–444.

Sambrook, J., E.F. Fritsch, and T. Maniatis. 1989. Molecular Cloning: A Laboratory Manual. Cold Spring Harbor Laboratory Press, Cold Spring Harbor, NY.

Sandrock, T.M., J.L. O'Dell, and A.E.M. Adams. 1997. Allele-specific suppression by formation of new protein-protein interactions in yeast. *Genetics.* 147:1635–1642.

Schafer, D.A., P.B. Jennings, and J.A. Cooper. 1996. Dynamics of capping protein and actin assembly in vitro: uncapping barbed ends by polyphosphoinositides. *J. Cell Biol.* 135:169–179.

Shaw, S.L., E. Yeh, P. Maddox, E.D. Salmon, and K. Bloom. 1997. Astral microtubule dynamics in yeast: a microtubule-based searching mechanism for spindle orientation and nuclear migration into the bud. *J. Cell Biol.* 139:985–994.

Stearns, T. 1997. Motoring to the finish: Kinesin and dynein work together to orient the yeast mitotic spindle. *J. Cell Biol.* 138:957–960.

Susuki, K., J. Nishihata, Y. Arai, N. Honma, K. Yamamoto, T. Irimura, and S. Toyoshima. 1995. Molecular cloning of a novel actin-binding protein, p57, with a WD repeat and a leucine zipper. *FEBS Lett.* 364:283–288.

Symons, M., J.M. Derry, B. Karlak, S. Jiang, V. Lemahieu, F. McCormick, U. Francke, and A. Abo. 1996. Wiskott-Aldrich syndrome protein, a novel effector for the GTPase CDC4211s, is implicated in actin polymerization. *Cell.* 84:723–734.

Terasaki, A.G., M. Ohnuma, and I. Mabuchi. 1997. Identification of actin-binding proteins from sea urchin eggs by F-actin affinity column chromatography. *J. Biochem.* 122:226–236.

Waddle, J.A., T.S. Karpova, R.H. Waterston, and J.A. Cooper. 1996. Movement of cortical actin patches in yeast. *J. Cell Biol.* 132:861–870.

Wall, M.A., D.E. Coleman, E. Lee, J.A. Iniguez-Lluhi, B.A. Posner, A.G. Gilman, and S.R. Sprang. 1995. The structure of the G protein heterotrimer $G_{i\alpha}\beta_1\gamma_2$. *Cell.* 83:1047–1058.

Wegner, A., and J. Engel. 1975. Kinetics of the cooperative association of actin and actin filaments. *Biophys. Chem.* 3:215–225.

Welch, M.D., A. Iwamatsu, and T.J. Mitchison. 1997. Actin polymerization is induced by Arp2/3 protein complex at the surface of *Listeria monocytogenes*. *Nature.* 385:265–268.

Welch, M.D., J. Rosenblatt, J. Skoble, D.A. Portnoy, and T.J. Mitchison. 1998. Interaction of human Arp2/3 complex and the *Listeria monocytogenes* ActA protein in actin filament nucleation. *Science.* 281:105–108.

Winter, D., A.V. Podtelejnikov, M. Mann, and R. Li. 1997. The complex containing actin-related protein Arp2 and Arp3 is required for the motility and integrity of yeast actin patches. *Curr. Biol.* 7:519–529.

Zaphiropoulos, P.G., and R. Toftgard. 1996. cDNA cloning of a novel WD repeat protein mapping to the 9q22.3 chromosomal region. *DNA Cell Biol.* 15:1049–1056.

Zechel, K. 1980. Isolation of polymerization-competent cytoplasmic actin by affinity chromatography on immobilized DNAse I using formamide as eluant. *Eur. J. Biochem.* 110:343–348.

Zigmond, S.H., M. Joyce, Y. Changsong, K. Brown, M. Huang, and M. Pring. 1998. Mechanism of Cdc42-induced actin polymerization in neutrophils extracts. *J. Cell Biol.* 142:1001–1012.

Zigmond, S.H. 1998. The arp2/3 complex gets to the point. *Curr. Biol.* 8:R654–R657.